Viral Load Is a Significant Prognostic Factor for Hepatitis B Virus-Associated Hepatocellular Carcinoma

Kazuaki Ohkubo, M.D.[1]
Yuji Kato, M.D.[1]
Tatsuki Ichikawa, M.D.[1]
Yuji Kajiya, M.D.[1]
Yoshio Takeda, M.D.[1]
Shinnichirou Higashi, M.D.[1]
Keisuke Hamasaki, M.D.[1]
Kazuhiko Nakao, M.D.[2]
Keisuke Nakata, M.D.[1]
Katsumi Eguchi, M.D.[1]

[1] The First Department of Internal Medicine, Nagasaki University School of Medicine, Nagasaki, Japan.

[2] Health Research Center, Nagasaki University School of Medicine, Nagasaki, Japan.

Address for reprints: Katsumi Eguchi, M.D., The First Department of Internal Medicine, Nagasaki University School of Medicine, 1-7-1 Sakamoto, Nagasaki 852-8501, Japan; Fax: (011) +81-95-849-7270; E-mail: f1072@cc.nagasaki-u.ac.jp.

Received August 8, 2001; revision received December 6, 2001; accepted December 17, 2001.

BACKGROUND. Hepatitis B virus (HBV) is closely linked to hepatocellular carcinoma (HCC). The objective of the current study was to identify the factors involved in the prognosis of patients with HBV-associated HCC using multivariate analysis.

METHODS. The current study included 74 patients with HBV-associated HCC who were admitted to Nagasaki University Hospital, Nagasaki, Japan, between 1983-1998. Of these, 13 patients underwent surgical tumor resection; 43 patients received nonsurgical treatment with transcatheter arterial embolization, percutaneous ethanol injection, or both; and 18 patients were followed without any active treatment. The significance of the patient's age; gender; history of blood transfusion; alcohol use; serum levels of alanine aminotransferase, α-fetoprotein, and HBV-DNA; number and size of liver tumors; clinical stage; and histologic diagnosis of HCC as prognostic factors was evaluated using univariate and multivariate analyses.

RESULTS. The 3-year, 5-year, and 10-year postdiagnosis cumulative survival rates were 36%, 21%, and 17%, respectively. Multivariate analysis identified the level of serum HBV-DNA and tumor size at diagnosis as independent and significant prognostic factors ($P = 0.0022$ and $P = 0.0106$, respectively). In addition, a low level of viremia was found to be associated with longer survival ($P = 0.0057$) even in patients who were negative for the hepatitis B e antigen.

CONCLUSIONS. The results of the current study suggest that viral load is a useful prognostic marker for HBV-related HCC and that HCC patients with a less favorable course appear either to clear the virus poorly or to have a greater level of virus production. *Cancer* **2002;94:2663–8.** © *2002 American Cancer Society.*
DOI 10.1002/cncr.10557

KEYWORDS: hepatocellular carcinoma (HCC), hepatitis B virus (HBV), HBV-DNA, prognosis.

Persistent hepatitis B virus (HBV) infection evolves into chronic hepatitis and cirrhosis. A portion of chronic cases progress to hepatocellular carcinoma (HCC), which is one of the most common malignancies worldwide, especially in several areas of Asia and Africa, where at least 250,000 cases of HCC are reported to occur annually. The relative risk of HBV carriers for HCC approaches 200:1, which to our knowledge is one of the highest relative risks known for a human malignancy.[1] In Japan, HCC currently is the third most common cancer in men and the fourth most common cancer in women, with an annual death rate that exceeds 30,000, although the recently reported increase in incidence of HCC is believed to be caused mainly by the increased number of patients with hepatitis C virus (HCV)-associated HCC.[2–5]

Advances in biotechnology permit the early recognition and treatment of HCC. However, in the most recent reports, the 3-year survival rate barely reached 40%. The low rate of survival after any treatment is, in part, due to the high incidence of recurrence and secondary primary tumor; in fact, the incidence is reported to be approximately 25% 1 year after radical surgical resection of the primary tumor and approximately 50% after 2 years.[6,7]

Several investigators have attempted to identify prognostic factors occurring in patients with HCC. In these studies, various clinicopathologic features of HCC such as the number and size of the liver tumors and the clinical stage of coexisting cirrhosis were linked to the survival rates of patients.[2,8-10] With regard to chronic HBV infection, recent studies have indicated that the serum level of HBV-DNA is correlated with progression of the disease.[11] However, to our knowledge only a few reports published to date have suggested a relation between viral status and prognosis in patients with HBV-associated HCC.[12] In the current study, univariate and multivariate analyses of the prognostic factors, including serum HBV-DNA, were performed in 74 patients with HBV-associated HCC. The results of analyses showed that the baseline level of HBV-DNA is a key factor in the prognosis of these patients.

MATERIALS AND METHODS

Patients

Four hundred four patients who were diagnosed with HCC histopathologically or clinically were admitted to Nagasaki University Hospital, Nagasaki, Japan, between 1983 and 1998. Of these, 74 patients (18%) who were positive for hepatitis B surface antigen (HBsAg) but negative for the antibody to HCV (anti-HCV) were enrolled in the current study. They included 55 men and 19 women ages 32–76 years. Sixty-five of these 74 patients had cirrhosis whereas the remaining patients had chronic hepatitis. The diagnosis of HCC was based on histopathologic findings of tumor tissue in 20 patients and on the characteristic appearance on ultrasonography, computed tomography, and hepatic arteriography in 54 patients. In the latter group, hepatic tumors demonstrated a hypervascularity on arteriography and/or the arterial phase on computed tomography. Of the 74 patients with HBV-associated HCC, 13 were treated with surgical resection of the liver tumors; 43 patients received nonsurgical treatment with transcatheter arterial embolization, percutaneous ethanol injection, or both; and 18 patients did not receive any active treatment. All patients were followed regularly in the study institution. The observation period began at the time of diagnosis and ended at the time of death or at the end of October 1999. No patient was lost to follow-up during the current study.

Viral Markers

After informed consent was obtained, a serum sample was obtained at the time of HCC diagnosis from each patient and was stored at −40 °C for later analysis of viral markers. HBsAg, hepatitis B e antigen (HBeAg), and anti-HBe were assayed by commercially available radioimmunoassay kits (Dainabot, Tokyo, Japan). Anti-HCV was determined using a second-generation or third-generation enzyme-linked immunoadsorbent assay (Ortho Diagnostics Systems, Tokyo, Japan). Serum HBV-DNA was detected by the transcription-mediated amplification (TMA) method as described previously,[13] and was expressed as the logarithm of genome equivalent per milliliter (LGE/mL). The detection limit of this method is 3.7 LGE/mL. The value of 0.7 milliequivalent per milliliter (mEq/mL), the detection limit of HBV-DNA by a branched DNA assay, corresponds to that of 5.8 LGE/mL using the TMA method.

Statistical Analysis

The survival rate after the diagnosis of HCC in 74 patients with HBV was evaluated using the Kaplan–Meier method, and comparisons between groups were performed with the log-rank test. The prognostic factors were investigated in each group by univariate and multivariate analysis. These included 11 variables determined at the time of diagnosis: age; gender; history of blood transfusion; alcohol use; serum levels of alanine aminotransferase (ALT), α-fetoprotein (AFP), and HBV-DNA; number and size of liver tumors; clinical stage stratified according to the criteria of the Liver Cancer Study Group of Japan;[3] and histologic diagnosis of HCC. ALT and AFP were assayed by commercially available enzymatic assay kits (Kanto Kagaku, Tokyo, Japan) and radioimmunoassay kits (Dainabot), respectively. The Cox proportional hazards model was used for multivariate analysis of prognostic factors. All 11 variables also were entered into a forward stepwise regression model, and only significant variables were entered in the multiple logistic regression models. All analyses were performed using a statistical software package (StatView version 5.0; SAS Institute Inc., Cary, NC). P values < 0.05 were considered to be statistically significant.

RESULTS

Prevalence of HBV and HCV in Patients with HCC

Four hundred four patients with HCC were admitted to the study institution between 1983 and 1998. Of the

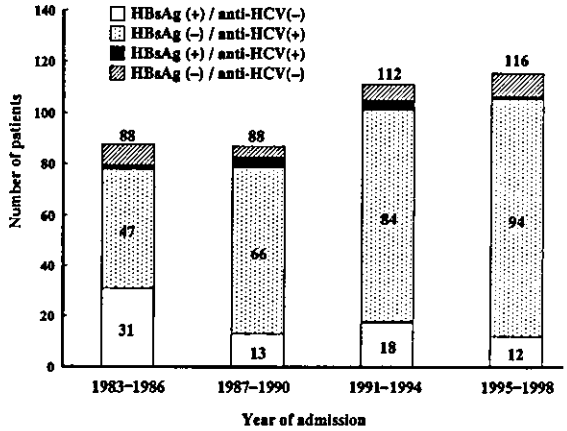

FIGURE 1. Serial changes in prevalence of hepatitis B virus (HBV) and hepatitis C virus (HCV) in patients with hepatocellular carcinoma during 1983–1998. A total of 404 patients with hepatocellular carcinoma were admitted to the study institution during this period. HBsAg: hepatitis B surface antigen; -: negative; +: positive.

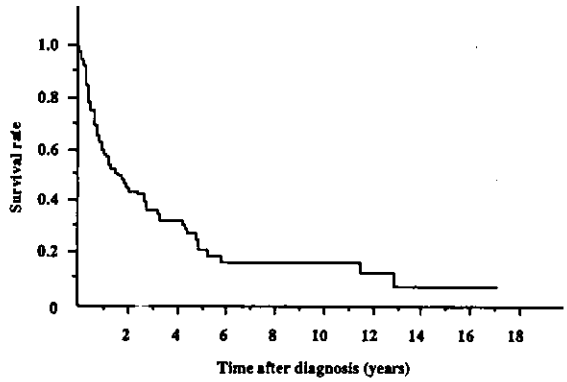

FIGURE 2. Cumulative survival curve of patients with hepatitis B virus-associated hepatocellular carcinoma. The cumulative survival of 74 patients after diagnosis was determined using the Kaplan–Meier method.

total of 404 patients, 74 (18%) were positive for HBsAg but negative for anti-HCV, 291 (72%) were negative for HBsAg but positive for anti-HCV, 12 (3%) were positive for both HBsAg and anti-HCV, and 27 (7%) were negative for both. The number of patients with HCC steadily increased during the observation period (Fig. 1). When serial changes in the prevalence of HBV and HCV in these patients were investigated, both the number and the proportion of patients with HCV successively increased during the time period studied. In contrast, the number of patients with HBV demonstrated a peak with 35% of patients with HCC reported between 1983–1986, followed thereafter by a relatively decreasing trend with a prevalence rate of 10% during 1995–1998.

Cumulative Survival of Patients with HBV-Associated HCC

The cumulative survival rate of 74 patients with HBV-associated HCC was evaluated using the Kaplan–Meier method (Fig. 2). The survival times of patients after diagnosis ranged from 1 month–17 years (median, 1.3 years). The 3-year, 5-year, and 10-year cumulative survival rates of the patients were 36%, 21%, and 17%, respectively.

Univariate Analysis of Prognostic Factors

To clarify the factors involved in the prognosis of patients with HBV-associated HCC, 11 variables present at the time of diagnosis of HCC were subjected to the univariate analysis using the Kaplan–Meier method coupled with the log-rank test (Table 1). Host-related factors such as age, gender, total alcohol intake until diagnosis, and history of blood transfusion did not appear to affect the cumulative survival of patients. In contrast, a serum HBV-DNA level < 3.7 LGE/mL ($P = 0.0002$) as well as a serum ALT level < 30 IU/L ($P = 0.0008$) at the time of diagnosis was found to be associated with significantly longer survival. Clinical stage of disease ($P = 0.0007$) also was found to be correlated with the cumulative survival rates of the patients. With regard to tumor-related factors, the serum AFP level did not appear to influence the survival time; however, the presence of a solitary tumor ($P = 0.0002$) and a tumor size < 2 cm in greatest dimension ($P = 0.0008$) were found to be linked closely to a favorable outcome. The histologic diagnosis of HCC did not appear to affect survival time.

Multivariate Analysis of Prognostic Factors

Multivariate analysis with a stepwise logistic regression model was performed using the same variables employed in the univariate analysis. Of the 11 variables, 2 factors (baseline level of HBV-DNA [$P = 0.0022$] and tumor size [$P = 0.0106$]) were identified as being significant prognostic factors for HCC in patients with HBV (Table 2). The serum level of HBV-DNA in patients with HCC who were positive for HBeAg was much higher than the value in those patients who were negative for HBeAg (median, 6.4 LGE/mL vs. 5.1 LGE/mL; $P < 0.0001$) (Fig. 3A). In addition, because HBeAg-positive patients with HCC had a poor prognosis compared with those patients who were negative for HBeAg, and because all patients who were positive for HBeAg had HBV-DNA levels ≥ 3.7 LGE/mL, the cumulative survival rates were

TABLE 1
Univariate Analysis of Prognostic Factors in Patients with HBV-Associated HCC

Variables	No.	Median survival time (yrs)	P value
Age (yrs)			
< 60	55	3.2	0.2092
≥ 60	19	1.2	
Gender			
Male	55	1.8	0.7054
Female	19	1.3	
History of blood transfusion			
Yes	13	0.8	0.7556
No	59	1.7	
Not assessed	2		
Alcohol use*			
< 500 kg	43	1.3	0.8447
≥ 500 kg	28	1.5	
Not assessed	3		
Serum HBV-DNA			
< 3.7 LGE/mL	15	5.8	0.0002
≥ 3.7 LGE/mL	53	1.2	
Not assessed	6		
Serum ALT			
< 30 IU/L	24	4.9	0.0008
≥ 30 IU/L	48	0.9	
Not assessed	2		
Clinical Stage			
I	39	3.2	0.0007
II or III	33	0.9	
Not assessed	2		
Serum α-fetoprotein			
< 200 ng/mL	36	2.4	0.2741
≥ 200 ng/mL	36	1.2	
Not assessed	2		
Liver tumor			
Solitary	37	4.3	0.0002
Multiple	37	0.7	
Tumor size			
< 2 cm	28	4.9	0.0008
≥ 2 cm	46	1.0	
Histologic diagnosis of HCC			
Yes	20	1.9	0.2977
No	54	1.2	
Not assessed	0		

HBV: hepatitis B virus; HCC: hepatocellular carcinoma; ALT: alanine aminotransferase. LGE/mL: logarithm of genome equivalent per milliliter;
*Total amount of alcohol intake before the diagnosis of hepatocellular carcinoma.

compared between HBeAg-negative patients who had HBV-DNA levels ≥ 3.7 LGE/mL (median, 5.9 LGE/mL) and those patients with levels < 3.7 LGE/mL (Fig. 3B). The cumulative survival curves apparently were different between the 2 groups ($P = 0.0057$), indicating that the baseline level of serum HBV-DNA did influence the survival time of patients with HBV-associated HCC, even those patients with HBeAg-negative disease.

TABLE 2
Independent Prognostic Factors in Patients with HBV-Associated HCC

Variables	Coefficient	Standard error	Chi-square	P value
Tumor size < 2 cm	0.826	0.323	6.534	0.0106
Serum HBV-DNA < 3.7 LGE/mL	1.355	0.442	9.386	0.0022

HBV: hepatitis B virus; HCC: hepatocellular carcinoma; LGE/mL: logarithm of genome equivalent per milliliter.

DISCUSSION

Epidemiologic studies estimate the annual incidence of HCC in patients who are chronically infected with HBV to be approximately 800 per 100,000. Although HCC has different manifestations in different parts of the world, the prognosis of untreated patients is very unfavorable with a median survival time of < 6 months.[1,14] Given the high frequency and mortality of HCC, elucidation of the mechanisms by which HBV participates in the process of chronic liver disease, including HCC, will have a profound impact on the prevention and treatment of chronic HBV infections.

In the current study, the number of patients with HCC recently increased mainly due to the increased number of patients with HCV, whereas the number of patients with HBV was nearly unchanged in the last 10 years. Similar results have been described elsewhere in Japan, as well as in Europe and the U.S.[2,4,10,14] Several lines of evidence indicate that type 1 interferon (IFN) treatment can inhibit the development of HCC in patients with chronic HCV infection, suggesting that clearance of the infected virus could have some beneficial effects on hepatocarcinogenesis.[15,16]

Previous studies have described the factors involved in the prognosis of patients with chronic HBV infection. Of these, seroconversion from HBeAg to anti-HBe is believed to result in a decrease in viral load and to indicate a favorable outcome in these patients.[1,2,12,17,18] However, recent advances in molecular technology have allowed the isolation of HBV variants that either cannot produce HBeAg or produce it less efficiently based on precore stop codon mutation and mutations in the core promoter region, respectively. In patients with HBV variants, progressive liver damage occurs in parallel with relatively high levels of viremia.[11] In the current study, the cumulative survival curve of 74 patients with HBV-associated HCC after diagnosis was nearly similar to those reported recently from Japan and other countries.[2,14,19] Among the prognostic factors analyzed, a serum HBV-DNA level of < 3.7 LGE/mL at the time of diagnosis of

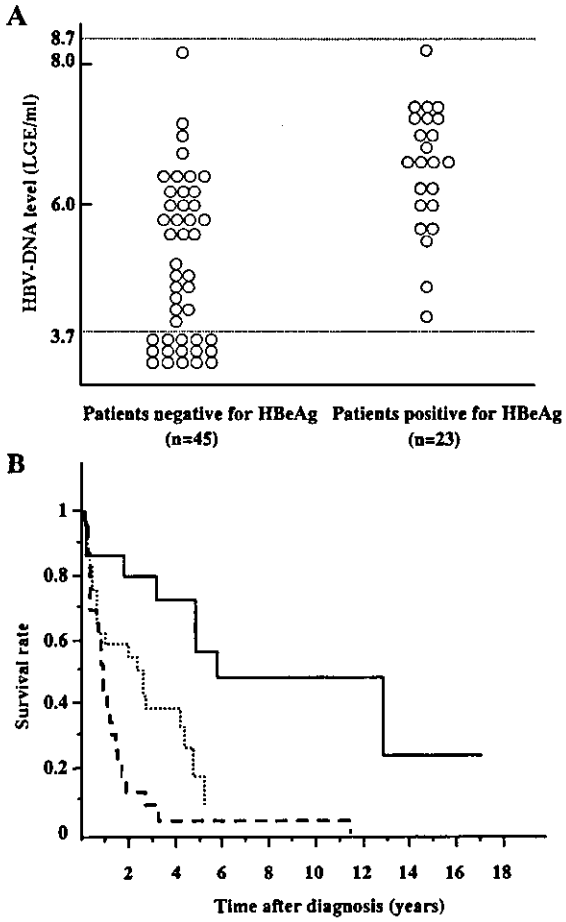

FIGURE 3. Effect of viral status on prognosis of patients with hepatitis B virus (HBV)-associated hepatocellular carcinoma. Serum samples were available for 68 patients for tests of both serum HBV-DNA and hepatitis B e antigen (HbeAg). (A) The viral load was associated closely with the presence or absence of HBeAg ($P < 0.001$). The dotted lines represent the upper and lower detection limits of HBV-DNA measured by the transcription-mediated amplification method, respectively. (B) The cumulative survival rate of HBeAg-negative patients who had a serum HBV-DNA level < 3.7 logarithm of genome equivalent per milliliter (LGE/mL) ($n = 15$) (solid line) was significantly higher than that of HBeAg-negative patients who had detectable levels of HBV-DNA ($n = 30$) (dotted line) and that of HBeAg-positive patients ($n = 23$) (broken line) ($P < 0.01$, respectively).

HCC was found to be linked closely to a longer cumulative survival time in patients based on both univariate and multivariate analyses. Even by comparison with HBeAg-negative HCC patients, a low level of viremia represented a favorable outcome. Although other factors such as serum ALT, clinical stage of coexisting cirrhosis, and the number and size of the liver tumors were found to influence survival rates of patients on univariate analysis, multivariate analysis identified the baseline level of HBV-DNA, together with tumor size, to be an independent prognostic factor for HCC in patients with HBV. This is in agreement with the results described by Kubo et al.,[12] in which a high viral load was found to be associated with a high recurrence rate of HCC after surgical resection in patients with HBV. Conversely, the treatment was based on clinical stage as well as tumor size and number and, therefore, no independent effect of treatment was observed in the current study.

HBV-DNA sequencing using HCC tissue and adjacent nontumorous liver tissue has demonstrated a high rate of mutations in the X gene, a product of which is likely to play a crucial role in the pathogenesis of chronic infections and the development of HCC.[1,20–22] Because this region overlaps with the core promoter sequence, the mutations are recognized not only to induce a functional alteration of HBX but also to affect its transactivating ability. Although the significance of this finding is not yet known, active replication of the HBV variants in hepatocytes might be relevant to the development of HCC and tumor recurrence after treatment in patients with HBV. In addition, some investigators suggest that active hepatitis is a risk factor for HCC recurrence after surgical resection in patients with HBV.[6,7,12] In patients with HBeAg-negative disease, active hepatitis usually occurs in those who have relatively high levels of viremia containing the viral population of HBV variants.[11] Thus, it is conceivable that patients with a high viral load may have a high potential for hepatocarcinogenesis even after surgical or nonsurgical treatment of HCC.

The effectiveness of type 1 IFN treatment in patients with chronic HBV infection has been studied widely, and improvement of biochemical, virologic, and histopathologic markers by IFN treatment has been confirmed in patients with HBV.[16,23,24] Moreover, antiviral treatments with nucleoside analogues such as lamivudine and adefovir recently have been implemented in patients with HBV. These agents modulate the replicative activities of the infected virus in hepatocytes. In clinical trials, the oral administration of these agents in patients with HBV was reported to reduce the serum level of HBV-DNA, and also was found to result in biochemical and, in part, histopathologic improvements.[25–28] In the current study, viral load was found to be a key prognostic factor for HCC in patients with HBV. Although the independent role of the level of viremia observed in the current study must be validated by further investigations, antiviral treatment in combination with the surgical or

nonsurgical treatment of HCC will be a promising treatment strategy for the disease.

REFERENCES

1. Feitelson MA, Duan LX. Hepatitis B virus x antigen in the pathogenesis of chronic infections and the development of hepatocellular carcinoma. *Am J Pathol.* 1997;150:1141–1157.
2. Shiratori Y, Shiina S, Imamura M, et al. Characteristic difference of hepatocellular carcinoma between hepatitis B- and C- viral infection in Japan. *Hepatology.* 1995;22:1027–1033.
3. The Liver Cancer Study Group of Japan. Primary liver cancer in Japan. Clinicopathologic features and results of surgical treatment. *Ann Surg.* 1990;211:277–287.
4. Ikeda K, Saitoh S, Koida I, et al. A multivariate analysis of risk factors for hepatocellular carcinogenesis: a prospective observation of 795 patients with viral and alcoholic cirrhosis. *Hepatology.* 1993;18:47–53.
5. Tanaka K, Ikematsu H, Hirohata T, Kashiwagi S. Hepatitis C virus infection and risk of hepatocellular carcinoma among Japanese: possible role of type 1b (II) infection. *J Natl Cancer Inst.* 1996;88:742–746.
6. Lise M, Bacchetti S, Da Pian P, Nitti D, Pilati PL, Pigato P. Prognostic factors affecting long term outcome after liver resection for hepatocellular carcinoma. *Cancer.* 1998;82:1028–1036.
7. Poon RT, Fan ST, Ng IO, Lo CM, Liu CL, Wong J. Different risk factors and prognosis for early and late intrahepatic recurrence after resection of hepatocellular carcinoma. *Cancer.* 2000;89:500–507.
8. Chin PL, Chu DZ, Clarke KG, Odem-Maryon T, Yen Y, Wagman LD. Ethnic differences in the behavior of hepatocellular carcinoma. *Cancer.* 1999;85:1931–1936.
9. Shirabe K, Shimada M, Kajiyama K, et al. Clinicopathologic features of patients with hepatocellular carcinoma surviving > 10 years after hepatic resection. *Cancer.* 1998;83:2312–2316.
10. Stuart KE, Anand AJ, Jenkins RL. Hepatocellular carcinoma in the United States: prognostic features, treatment outcome, and survival. *Cancer.* 1996;77:2217–2222.
11. Kajiya Y, Hamsaki K, Nakata K, et al. A long-term follow-up analysis of serial core promoter and precore sequences in Japanese patients chronically infected by hepatitis B virus. *Dig Dis Sci.* 2001;46:509–515.
12. Kubo S, Hirohashi K, Tanaka H, et al. Effect of viral status on recurrence after liver resection for patients with hepatitis B virus-related hepatocellular carcinoma. *Cancer.* 2000;88:1016–1024.
13. Kamisango K, Kamogawa C, Sumi M, et al. Quantitative detection of hepatitis B virus by transcription-mediated amplification and hybridization protection assay. *J Clin Microbiol.* 1999;37:310–314.
14. Di Bisceglie AM, Carithers RL, Gores GJ. Hepatocellular carcinoma. *Hepatology.* 1998;28:1161–1165.
15. Ikeda K, Saitoh S, Arase Y, et al. Effect of interferon therapy on hepatocellular carcinogenesis in patients with chronic hepatitis type C: a long-term observation study of 1,643 patients using statistical bias correction with proportional hazard analysis. *Hepatology.* 1999;29:1124–1130.
16. Lin SM, Sheen IS, Chien RN, Chu CM, Liaw YF. Long-term beneficial effect of interferon therapy in patients with chronic hepatitis B virus infection. *Hepatology.* 1999;29:971–975.
17. Fattovich G, Rugge M, Brollo L, et al. Clinical, virologic and histologic outcome following seroconversion from HBeAg to anti-HBe in chronic hepatitis type B. *Hepatology.* 1986;6:167–172.
18. Di Marco V, Lo Iacono O, Camma C, et al. The long-term course of chronic hepatitis B. *Hepatology.* 1999;30:257–264.
19. Kato Y, Hamasaki K, Aritomi T, Nakao K, Nakata K, Eguchi K. Most of the patients with cirrhosis in Japan die from hepatocellular carcinoma. *Oncol Rep.* 1999;6:1273–1276.
20. Kim CM, Koike K, Saito I, Miyamura T, Jay G. HBx gene of hepatitis B virus induces liver cancer in transgenic mice. *Nature.* 1991;351:317–320.
21. Wang XW, Gibson MK, Vermeulen W, et al. Abrogation of p53-induced apoptosis by the hepatitis B virus X gene. *Cancer Res.* 1995;55:6012–6016.
22. Paterlini P, Poussin K, Kew M, Franco D, Brechot C. Selective accumulation of the X transcript of hepatitis B virus in patients negative for hepatitis B surface antigen with hepatocellular carcinoma. *Hepatology.* 1995;21:313–321.
23. Niederau C, Heintges T, Lange S, et al. Long-term follow-up of HBeAg-positive patients treated with interferon alfa for chronic hepatitis B. *N Engl J Med.* 1996;334:1422–1427.
24. Brunetto MR, Oliveri F, Colombatto P, Capalbo M, Barbera C, Bonino F. Treatment of chronic anti-HBe-positive hepatitis B with interferon-alfa. *J Hepatol.* 1995;22:42–44.
25. Farrell GC. Clinical potential of emerging new agents in hepatitis B. *Drugs.* 2000;60:701–710.
26. Leung N. Nucleoside analogues in the treatment of chronic hepatitis B. *J Gastroenterol Hepatol.* 2000;15:E53–E60.
27. Perrillo R, Schiff E, Yoshida E, et al. Adefovir dipivoxil for the treatment of lamivudine-resistant hepatitis B mutants. *Hepatology.* 2000;32:129–134.
28. Suzuki Y, Kumada H, Ikeda K, et al. Histological changes in liver biopsies after one year of lamivudine treatment in patients with chronic hepatitis B infection. *J Hepatol.* 1999;30:743–748.

ACADEMIC PRESS

Biochemical and Biophysical Research Communications 294 (2002) 414–422

BBRC

www.academicpress.com

Involvement of IL-1β and IL-10 in IFN-α-mediated antiviral gene induction in human hepatoma cells☆

Tatsuki Ichikawa,[a] Kazuhiko Nakao,[b] Keisuke Nakata,[a] Mayumi Yamashita,[c] Keisuke Hamasaki,[a] Masaya Shigeno,[a] Seigou Abiru,[a] Hiroki Ishikawa,[a] Nobuko Ishii,[b] and Katsumi Eguchi[a,*]

[a] *The First Department of Internal Medicine, Nagasaki University School of Medicine, 1-7-1 Sakamoto, Nagasaki 852-8501, Japan*
[b] *Health Research Center, Nagasaki University, Nagasaki, Japan*
[c] *Department of Clinical Pharmacology, Nagasaki University, Nagasaki, Japan*

Received 7 May 2002

Abstract

Crosstalk between interferons (IFNs) and several cytokines is likely to play an important role in viral clearance in chronic hepatitides B and C. We investigated the influence of this phenomenon on IFN-inducible antiviral gene expression in HuH-7 human hepatoma cells. HuH-7 cells were treated with IFN-α in the absence or presence of interleukin-1β (IL-1β) or IL-10 and the expression of antiviral genes such as 2′5′-oligoadenylate synthetase (2′5′-OAS) and double-stranded RNA-dependent protein kinase (PKR), as well as activation of signal transducer and activator of transcription 1 (STAT1), a key step for relaying the IFN-α signals, was analyzed by Northern blotting, Western blotting, and the reporter gene transfection assay. IL-1β potentiated IFN-α-induced 2′5′-OAS and PKR gene expression, similar to expression of the transfected reporter genes containing the IFN-stimulated regulatory elements, while IL-10 suppressed IFN-α-stimulated gene expression. With regard to IFN-α signaling, IL-1β enhanced both tyrosine and serine phosphorylation of STAT1 through p38 mitogen-activated protein kinase activation. In contrast, IL-10 inhibited IFN-α-mediated tyrosine phosphorylation of STAT1 by induction of a Janus kinase inhibitor, JAB. IL-1β and IL-10 interact with IFN-α to up- and down-regulate antiviral gene expression, respectively, by modulating STAT1 activation induced by IFN-α.

Keywords: Hepatitis C; Hepatitis B; IFN, IL-1β; IL-10; Cytokines; Crosstalk; STAT

Hepatitis B virus (HBV) and hepatitis C virus (HCV) cause chronic hepatitis and liver cirrhosis and are closely linked to the development of hepatocellular carcinoma. Interferon-α (IFN-α) has been used as an antiviral agent against HBV and HCV and leads to clinical improvement in patients with chronic hepatitides B and C [1,2]. However, more than a half of patients show only transient or no response to IFN-α therapy [3,4].

After binding to its receptor, IFN-α stimulates the intracellular IFN signaling cascade including the activation of receptor-associated Janus tyrosine kinases (JAK) 1 and Tyk2, followed by phosphorylation of signal transducers and activators of transcription 1, 2 (STAT1, STAT2). The formed IFN-stimulated gene factor 3 (ISGF3), which consists of p48 and phosphorylated STAT1 and STAT2, translocates into the nucleus and binds to the IFN-stimulated regulatory element (ISRE) in the promoter sequences of a variety of IFN-inducible genes including antiviral proteins such as 2′5′-oligoadenylate synthetase (2′5′-OAS) and double-stranded RNA-dependent protein kinase (PKR) and *trans*-activates their gene transcription [5,6]. In this context, unresponsiveness or resistance to IFN-α treatment could be attributed to functional defects of

☆ *Abbreviations:* CIS, cytokine-inducible SH2 protein; EPO, erythropoietin; GM-CSF, granulocyte-macrophage colony stimulating factor; IFN, interferon; IL, interleukin; JAB, JAK binding protein; PBS, phosphate-buffered saline; SDS, sodium dodecyl sulfate; SOCS, suppressor of cytokine signaling; Th, T helper; Tyk, tyrosine kinase.

* Corresponding author. Fax: +81-95-849-7270.
E-mail address: eguchi@net.nagasaki-u.ac.jp (K. Eguchi).

0006-291X/02/$ - see front matter
PII: S0006-291X(02)00502-8

any signaling molecule involved in relaying the IFN-α signals.

Interleukin-1β (IL-1β), a proinflammatory cytokine mainly produced by monocytes and macrophages including Kupffer cells, is believed to play a crucial role in viral clearance and the host immune response to the virus. Previous studies have shown that the intrahepatic expression of IL-1β by sinusoidal lining cells is significantly lower in patients with chronic hepatitis C than in controls [7] and that the release of IL-1β and tumor necrosis factor-α (TNF-α) from peripheral blood monocytes following stimulation with phorbol ester is apparently reduced in chronic hepatitis C patients [8]. In case of chronic hepatitis B, Daniels et al. [9] reported that resolution of the disease during IFN-α treatment was accompanied by increased production of IL-1β and TNF-α. We also showed that IFN-α in combination with IL-1β produced a more profound suppression of the HBV enhancer-1 activity than IFN-α alone in human hepatoma cells [10,11]. These in vitro and in vivo studies suggest the cooperative effects of IL-1β on the IFN-mediated clearance of HBV and HCV.

Interleukin-10 (IL-10), identified as a Th2 cytokine, acts as a potent inhibitor of Th1 effector mechanisms. Activated monocytes are the main source of IL-10 production. However, Kupffer cells and stellate cells also produce IL-10 and this site of production probably participates directly in the process of immune-mediated viral eradication and liver inflammation [12–14]. In fact, spontaneous IL-10 production by peripheral blood mononuclear cells is greater in chronic hepatitis C patients than in controls and diminishes during IFN-α treatment [15]. Recent studies also suggest that patients who are genetically predisposed to IL-10 overproduction have a poor response to IFN-α treatment [16]. Thus, IL-10, in contrast to IL-1β, may function to repress the antiviral activities induced by IFNs in patients with HBV or HCV.

In the present study, we elucidated the roles of IL-1β and IL-10 in the expression of IFN-inducible antiviral genes such as 2′5′-OAS and PKR, by investigating their interactive effects on the IFN-α signaling cascade in HuH-7 human hepatoma cells.

Materials and methods

Reagents and cell culture. Recombinant human IFN-α 2a and IL-1β were gifts from Nippon Rosche (Tokyo, Japan) and Otsuka Pharmaceutical (Tokushima, Japan), respectively. Recombinant human IL-10 was obtained from Genzyme (Cambridge, MA). SB203580, a specific cell-permeable inhibitor of p38 mitogen-activated protein (MAP) kinase [17], and pyrrolidine dithiocarbamate (PDTC), which inhibits the nuclear translocation of nuclear factor-κB (NF-κB) but cannot inhibit the proteasome activity [18], were obtained from Calbiochem (San Diego, CA) and Sigma Chemical (St. Louis, MO), respectively. HuH-7 and HepG2 human hepatoma cells were maintained in a chemically defined medium, IS-RPMI, supplemented with 2% fetal bovine serum. In each experiment, the cells were cultured in serum-free IS-RPMI containing varying concentrations of IFN-α, IL-1β, and IL-10.

Northern blotting. Total cellular RNA was isolated by guanidium isothiocyanate method and 10 μg of RNA was size-fractionated on a 1% formaldehyde–agarose gel, transferred to a Hybound N nylon membrane (Amersham, UK), and hybridized with [^{32}P]-labeled cDNA probe. Human 2′5′-OAS cDNA probe used in this study was described previously [19]. Human β-actin cDNA probe (Wako Chemical, Osaka, Japan) was used as a control.

Western blotting and immunoprecipitation. Immunoblotting with anti-PKR, anti-STAT1 (Santa Cruz Biotechnology, Santa Cruz, CA), anti-tyrosine-701 phosphorylated STAT1 (New England Biolab, Beverly, MA), anti-serine-727 phosphorylated STAT1 (Upstate Biolab, Lake Placid, NY), or anti-human β-actin (Sigma) was performed as described previously [19]. Briefly, HuH-7 and HepG2 cells were lysed by addition of lysis buffer (50 mmol/L Tris–HCl, pH 7.4, 1% Np40, 0.25% sodium deoxycholate, 0.02% sodium azide, 0.1% SDS, 150 mmol/L NaCl, 1 mmol/L EDTA, 1 mmol/L PMSF, each of 1 μg/mL of aprotinin, leupeptin, and pepstatin, 1 mmol/L sodium *o*-vanadate, and 1 mmol/L NaF). Samples were analyzed by electrophoresis on 8–12% SDS–polyacrylamide gel, electrotransferred to nitrocellulose membranes, and then blotted with each antibody. The membranes were incubated with horseradish peroxidase-conjugated anti-rabbit IgG or anti-mouse IgG and the immunoreactive bands were visualized by the ECL chemiluminescence system (Amersham Life Science, Buckinghamshire, England). Similarly, expression of p38 MAP kinase and threonine-180/tyrosine-182 phosphorylated p38, as well as expression of JAB/SOCS-1 or CIS-3/SOCS-3 proteins, was determined using rabbit polyclonal antibodies recognizing each protein (anti-p38 and anti-phosphorylated p38, New England Biolab, Beverly, MA; anti-JAB and anti-SOCS-3, IBL, Fujioka, Japan). For analysis of JAK1 and STAT2 phosphorylation, samples were incubated with anti-JAK1 protein (Upstate Biolab, Lake Placid, NY) or anti-STAT2 (Santa Cruz Biotechnology, Santa Cruz, CA) at 4 °C for 8 h and treated with protein G–Sepharose beads (Pharmacia, Piscataway, NJ) at 4 °C for 2 h. After centrifugation, the beads were washed with PBS and boiled in gel electrophoresis sample buffer and then the immunoprecipitates were separated on 8% SDS–polyacrylamide gel, electrotransferred to nitrocellulose membrane, and blotted with anti-phosphotyrosine mouse monoclonal antibody (Upstate Biolab). For the control, the membrane was stripped and reprobed with anti-JAK1 or anti-STAT2.

Reporter gene transfection assay. pISRE–Luc containing five copies of the ISRE sequence and firefly luciferase gene and pRL-SV40 containing SV40 early enhancer/promoter and renilla luciferase gene were obtained from Clontech (San Diego, CA) and Promega (Madison, WI), respectively. The HuH-7 cells were grown in 24-well multiplates and transfected with 1 μg pISRE–Luc and 10 ng pRL-SV40 as a standard by the lipofection method. One day later, the cells were incubated in the absence or presence of varying concentrations of IFN-α, IL-1β, and IL-10 for 6 h and the luciferase activities in the cells were determined using a dual-luciferase reporter assay system and a TD-20/20 luminometer (Promega). Data were expressed as the relative ISRE–luciferase activity. In addition, pQ6A-CAT plasmid (a gift from Dr. N. Fujii, Sapporo Medical University, Sapporo, Japan), in which the 1.1 kb human 2′5′-OAS gene promoter containing the ISRE sequence, 5′-GAGGAAACGAAACC-3′ [20], is linked to chloramphenicol acetyltransferase (CAT) gene, was transfected into HuH-7 cells using 2 μg plasmid DNA per dish (25 cm^2) by the lipofection method. The cells were incubated in the absence or presence of 500 IU/mL IFN-α, 100 IU/mL IL-1β, 100 ng/mL IL-10 or IFN-α in combination with IL-1β or IL-10. One day later, the cells were harvested and lysed by five cycles of freezing and thawing. The lysate was heated at 63 °C for 10 min to inactivate deacetylase and centrifuged at 15,000 rpm for

5 min and the supernatant was used for determination of the CAT activity as described previously [11].

JAB/SOCS-1 expression vector (JAB pcDNA3) and CIS3/SOCS-3 expression vector (SOCS-3 pcDNA3) [21], which contain the full-length JAB cDNA and SOCS-3 cDNA, respectively, were provided by Dr. Yoshimura (Kyushu University, Fukuoka, Japan). The HuH-7 cells were cotransfected with the reporter gene (pISRE–Luc and pRL-SV40) and each expression vector. One day later, the cells were incubated in the absence or presence of 500 IU/mL IFN-α for 6 h, then, the relative ISRE–luciferase activities were determined.

Results

Effects of IL-1β and IL-10 on IFN-α-induced antiviral gene expression

HuH-7 cells were incubated in the absence or presence of IFN-α, IL-1β or a combination of both and total RNA was isolated from the cells before and 1, 2, 4, 8, and 24 h after stimulation. Northern blot analysis (Fig. 1A) showed that IFN-α stimulated the expression of 2′5′-OAS mRNA, which could be detected 4 h after stimulation as 1.6, 1.8, and 3.6 kb mRNA in length, as reported previously [22], and reached a peak level at 8–24 h. In contrast, IL-1β did not induce the expression

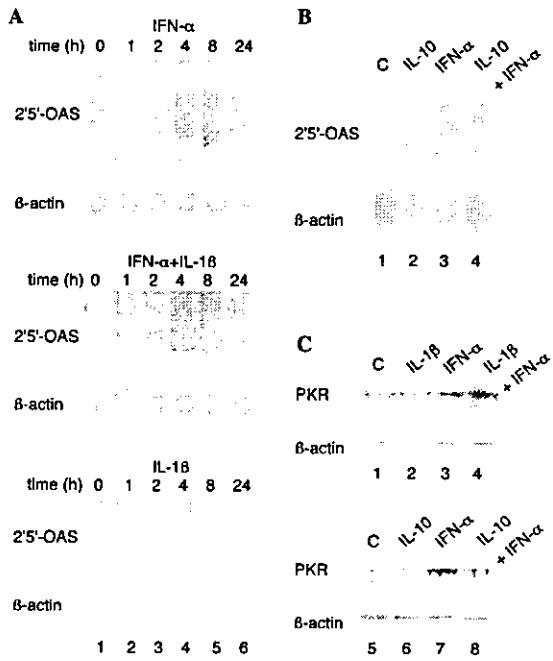

Fig. 1. Effects of IL-1β and IL-10 on IFN-α-induced 2′5′-OAS and PKR expression. (A) HuH-7 cells were incubated in the absence or presence of 500 IU/mL IFN-α, 100 IU/mL IL-1β or both, and total cellular RNA (10 μg) isolated at the indicated times was analyzed for 2′5′-OAS mRNA or β-actin mRNA as a control by Northern blotting. (B) HuH-7 cells were incubated in the absence (lane 1) or presence of 100 ng/mL IL-10 (lane 2), 500 IU/mL IFN-α (lane 3) or both (lane 4). One day later, 2′5′-OAS mRNA or β-actin mRNA as a control was nalyzed by Northern blotting. (C) HuH-7 cells were untreated (lanes 1 and 5) or treated with 100 IU/mL IL-1β (lane 2), 500 IU/mL IFN-α (lane 3) or both (lane 4) or treated with 100 ng/mL IL-10 (lane 6), 500 IU/mL IFN-α (lane 7) or both (lane 8). One day later, PKR expression was determined by Western blotting.

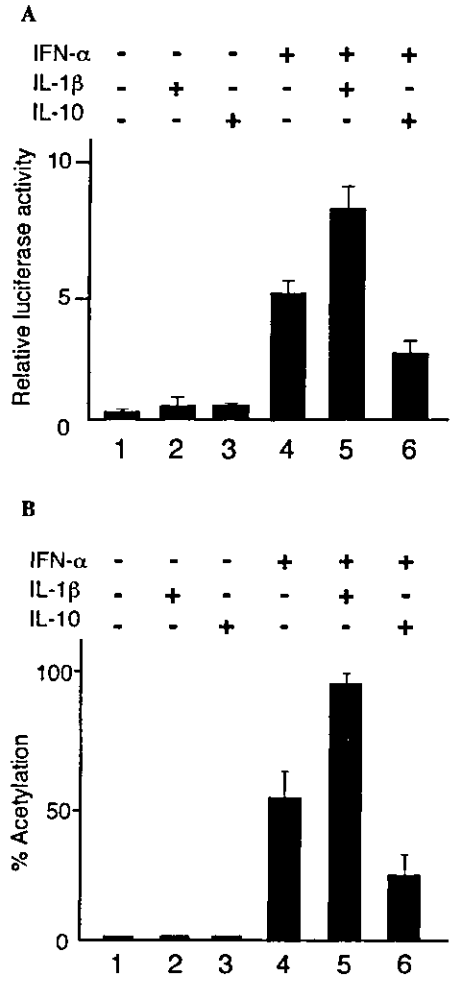

Fig. 2. Effects of IL-1β and IL-10 on IFN-α-induced activation of transfected reporter gene expression. (A) HuH-7 cells transfected with the reporter gene (pISRE–Luc and pRL-SV40 as a standard) were untreated (lane 1) or treated with 100 IU/mL IL-1β (lane 2), 100 ng/mL IL-10 (lane 3), 500 IU/mL IFN-α (lane 4) or IFN-α in combination with IL-1β (lane 5) or IL-10 (lane 6). Six hours later, the relative ISRE–luciferase activities ($n = 4$) were determined as described in Materials and methods. Data are expressed as means ± SD and are representative examples of three similar experiments. (B) HuH-7 cells were transfected with pQ6A-CAT plasmid and incubated in the absence (lane 1) or presence of 100 IU/mL IL-1β (lane 2), 100 ng/mL IL-10 (lane 3), 500 IU/mL IFN-α (lane 4) or IFN-α in combination with IL-1β (lane 5) or IL-10 (lane 6). One day later, CAT expression was determined as described in Materials and methods. The amounts of extract and incubation times were 15 μg protein and 30 min, respectively. CAT activity (percentage of acetylation) is expressed as mean ± SD of four separate experiments.

of 2′5′-OAS mRNA. However, when the cells were treated with both IFN-α and IL-1β, induction of the 2′5′-OAS mRNA was detected 1 h after stimulation and the peak level was clearly higher than that induced by IFN-α alone. To determine whether IL-10 influences the IFN-α-mediated 2′5′-OAS mRNA induction, HuH-7 cells were treated with IFN-α, IL-10 or both and total cellular RNA was isolated 24 h after stimulation. In contrast to IL-1β, IL-10 repressed the IFN-α-stimulated 2′5′-OAS mRNA expression (Fig. 1B).

In addition to 2′5′-OAS, PKR is a well-known IFN-α-inducible antiviral protein. Accordingly, we evaluated the interactive effects of IL-1β and IL-10 on the IFN-α-induced PKR expression. Western blot analysis (Fig. 1C) showed detectable levels of PKR expression in untreated HuH-7 cells, as described previously [19], and IFN-α up-regulated PKR expression. Furthermore, IL-1β augmented the IFN-α-mediated PKR induction, while IL-10 suppressed its induction, although IL-1β or IL-10 alone did not affect PKR expression.

Alterations of IFN-α-stimulated reporter gene expression by IL-1β and IL-10

Since the formation of ISGF3 by IFN-α leads to transactivation of the ISRE in the promoter regions of the IFN-α-inducible genes, we performed the reporter gene transfection assay using plasmids containing ISRE in their promoter sequences. HuH-7 cells were transfected with pISRE–Luc containing five repeats of the ISRE sequence and pRL-SV40 as a standard and then were treated with IFN-α in the absence or presence of IL-1β or IL-10. IL-1β and IL-10 alone did not influence the ISRE–luciferase activities (Fig. 2A). IFN-α stimulated the reporter gene expression and IFN-α combined with IL-1β further stimulated its expression compared with IFN-α alone. In contrast, IL-10 suppressed the stimulatory effect of IFN-α on the reporter gene expression.

pQ6A-CAT contains the 2′5′-OAS gene promoter linked to the CAT gene. Since the 2′5′-OAS gene transcription is mainly regulated by transactivation of ISRE in its promoter region, HuH-7 cells were transfected with pQ6A-CAT and treated with IFN-α in the absence or presence of IL-1β and IL-10. IFN-α-stimulated CAT expression from pQ6A-CAT, and addition of IL-1β or IL-10, similar to the results of the pISRE–Luc transfection assay, resulted in augmentation and suppression of the IFN-α-induced CAT expression, respectively (Fig. 2B).

Stimulatory effect of IL-1β on IFN-α-induced STAT1 protein activation

Activation of STAT1 protein by phosphorylation at tyrosine-701 residue is essential for the relay of IFN-α signals with the formation of ISGF3. In the next experiment, we determined the effect of IL-1β on the IFN-α-induced STAT1 phosphorylation by Western blotting. IFN-α clearly induced the tyrosine phosphorylation of STAT1 in HuH-7 cells, but IL-1β could not. However, when the cells were treated with both IFN-α and IL-1β, the levels of tyrosine phosphorylated STAT1 were apparently higher than those induced by IFN-α alone during the observation period (Fig. 3A). In addition, STAT1 remained phosphorylated 8 h after stimulation with IFN-α and IL-1β, while STAT1 phosphorylation decreased to undetectable levels at that time by IFN-α monotherapy. Similarly, IL-1β aug-

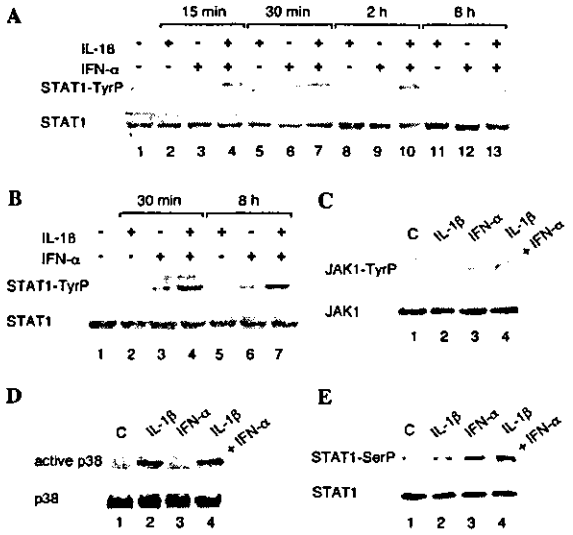

Fig. 3. Effects of IL-1β and IFN-α on STAT1, JAK1, and p38 MAP kinase activation. (A) HuH-7 cells were untreated (lane 1) or treated with 100 IU/mL IL-1β (lanes 2, 5, 8, and 11), 500 IU/mL IFN-α (lanes 3, 6, 9, and 12) or both (lanes 4, 7, 10, and 13) for the indicated periods and expression of STAT1 protein (lower panel) and the phosphorylated STAT1 at tyrosine-701 residue (upper panel) was analyzed by Western blotting. (B) HepG2 cells were untreated (lane 1) or treated with 100 IU/mL IL-1β (lanes 2 and 5), 500 IU/mL IFN-α (lanes 3 and 6) or both (lanes 4 and 7) for the indicated periods, and expression of STAT1 protein (lower panel) and the phosphorylated STAT1 at tyrosine-701 residue (upper panel) was analyzed by Western blotting. (C) HuH-7 cells were untreated (lane 1) or treated with 100 IU/mL of IL-1β (lane 2), 500 IU/mL IFN-α (lane 3) or both (lane 4) for 30 min, and the cell lysates were immunoprecipitated with anti-JAK1 protein, and the immunoprecipitates were blotted with anti-phosphotyrosine for the analysis of phosphorylated JAK1 at tyrosine-1022/-1023 residues (upper panel), then the membrane was stripped and reprobed with anti-JAK1 protein (lower panel). (D) HuH-7 cells were incubated in the absence (lane 1) or presence of similar amounts of IL-1β (lane 2), IFN-α (lane 3) or both (lane 4) for 30 min for Western blot analysis of p38 protein (lower panel) and the phosphorylated p38 at threonine-180/tyrosine-182 residues (upper panel). (E) HuH-7 cells were incubated in the absence (lane 1) or presence of similar amounts of IL-1β (lane 2), IFN-α (lane 3) or both (lane 4) for 30 min. Expression of STAT1 protein (lower panel) and the phosphorylated STAT1 at serine-727 residue (upper panel) was analyzed by Western blotting.

mented the levels of tyrosine phosphorylated STAT1 induced by IFN-α in HepG2 cells (Fig. 3B). On the other hand, IL-1β had no effect on the IFN-α-induced tyrosine phosphorylation of STAT2 in both cells (data not shown). In the IFN-α signaling cascade, STAT1 phosphorylation is induced by JAK1 activation. In fact, JAK1 phosphorylation at tyrosine-1022/1023 residues was found in response to IFN-α stimulation in this study. However, IL-1β did not enhance the level of phosphorylated JAK1 induced by IFN-α in HuH-7 (Fig. 3C). Recently, Bode et al. [23] demonstrated that p38 MAP kinase can mediate STAT1 tyrosine phosphorylation independent of the IFN-α signaling pathways. Therefore, we investigated whether IL-1β could cause p38 activation. Western blotting showed that IL-1β, as well as IL-1β combined with IFN-α, induced p38 activation, which was manifested by the appearance of phosphorylated p38, while IFN-α alone could not (Fig. 3D). Since p38 MAP kinase is also known to play a role in the phosphorylation of STAT1 at serine-727 residue [17], we examined whether IL-1β could stimulate the IFN-α-induced serine phosphorylation of STAT1. IFN-α induced the serine phosphorylation of STAT1 and IL-1β alone induced it weakly. However, when the HuH-7 cells were treated with both IFN-α and IL-1β, the levels of serine phosphorylated STAT1 were apparently higher than those induced by IFN-α alone (Fig. 3E). Next, we investigated whether addition of a specific p38 inhibitor, SB203580, could inhibit the tyrosine phosphorylation of STAT1 and activation of transfected ISRE–Luc gene, which were induced by treatment with IL-1β and IFN-α. Pretreatment with SB203580 but not PDTC, a selective NF-κB inhibitor used as a control, reduced the level of tyrosine phosphorylated STAT1 induced by combined treatment of IL-1β and IFN-α to the level induced by IFN-α alone (Fig. 4A). Consistent with this finding, functional analysis showed that the addition of SB203580 abrogated the stimulatory effect of IL-1β on IFN-α-induced reporter gene activation, whereas addition of PDTC did not have such effect (Fig. 4B).

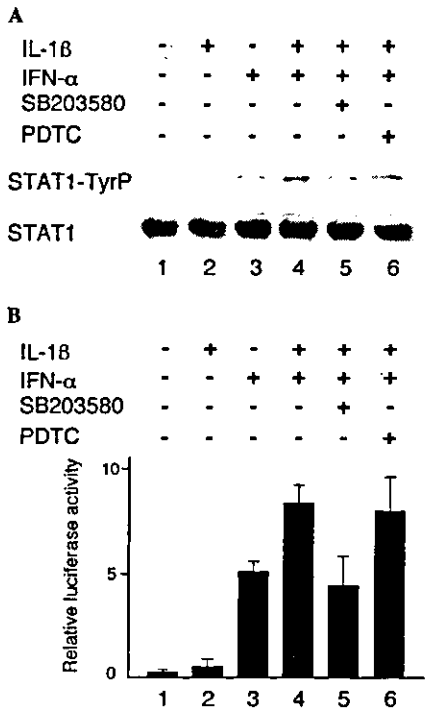

Fig. 4. Suppression of IFN-α/IL-1β-induced phosphorylation of STAT1 and activation of transfected reporter gene by SB203580, a specific p38 inhibitor. (A) HuH-7 cells were incubated in the absence (lane 1) or presence of 100 IU/mL IL-1β (lane 2), 500 IU/mL IFN-α (lane 3) or both (lane 4), or the cells were pretreated for 30 min with 20 μM of SB203580 or 100 μM of PDTC as a control, followed by treatment with both IL-1β and IFN-α for 30 min (lanes 5 and 6, respectively) for Western blot analysis of STAT1 protein (lower panel) and phosphorylated STAT1 at tyrosine-701 residue (upper panel). (B) HuH-7 cells transfected with the reporter gene (pISRE–Luc and pRL-SV40) were untreated (lane 1) or treated with 100 IU/mL IL-1β (lane 2), 500 IU/mL IFN-α (lane 3) or both (lane 4), or the cells were pretreated with SB203580 or PDTC, followed by treatment with both IL-1β and IFN-α (lanes 5 and 6, respectively). Six hours later, the relative ISRE–luciferase activity ($n = 4$) was determined as described in Materials and methods. Data are expressed as means ± SD and are representative examples of three similar experiments.

Inhibitory effect of IL-10 on IFN-α-induced STAT1 protein activation

In contrast to IL-1β, IL-10 suppressed the IFN-α-inducible antiviral gene expression. To elucidate the mechanisms by which IL-10 interacts with IFN-α signaling pathways, we investigated the effect of IL-10 on the IFN-α-induced tyrosine phosphorylation of STAT1. IFN-α caused the tyrosine phosphorylation of STAT1, but the addition of IL-10 dose-dependently suppressed the levels of tyrosine phosphorylated STAT1 induced by IFN-α (Fig. 5A). Whereas, IL-10 had no effect on the IFN-α-induced tyrosine phosphorylation of STAT2 (data not shown). Since the CIS family of proteins including JAB/SOCS-1 and CIS-3/SOCS-3 accounts for the negative regulation of JAK–STAT signaling in IFN-mediated pathways [24], we evaluated the effects of JAB and SOCS-3 on IFN-α-induced activation of the transfected ISRE–Luc gene. JAB gene transfection, as well as SOCS-3 gene transfection, dose-dependently suppressed IFN-α-activated ISRE–luciferase gene expression, although JAB was more efficient than SOCS-3 (Fig. 5B). To investigate whether IL-10 could induce JAB or SOCS-3 proteins in HuH-7 cells, Western blotting was performed using antibodies that recognize each protein. IL-10 induced JAB protein expression, which was detected 30 min after stimulation and increased up to 8 h after stimulation (Fig. 6A). SOCS-3 protein was expressed at baseline in HuH-7 cells, but IL-10 failed

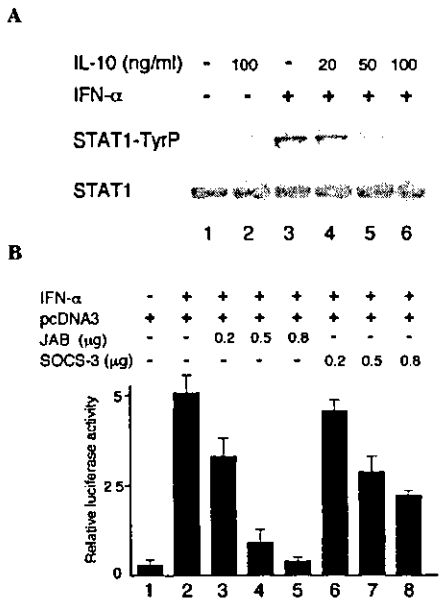

Fig. 5. Inhibitory effects of IL-10 and overexpression of JAB/SOCS-1 or CIS-3/SOCS-3 on IFN-α-induced STAT1 phosphorylation and reporter gene expression. (A) HuH-7 cells were untreated (lane 1) or treated with 100 ng/mL IL-10 (lane 2) or 500 IU/mL IFN-α in the absence (lane 3) or presence of 20, 50, and 100 ng/mL IL-10 (lanes 4, 5, and 6, respectively) for 30 min for Western blot analysis of STAT1 protein (lower panel) and the phosphorylated STAT1 at tyrosine-701 residue (upper panel). (B) HuH-7 cells were cotransfected with the reporter gene (pISRE–Luc and pRL-SV40) and a total of 1 μg of plasmids containing vehicle vector (pcDNA3) and JAB or SOCS-3 expression vector (JAB pcDNA and SOCS-3 pcDNA, respectively) at different proportions. One day later, the cells were incubated in the absence or presence of 500 IU/mL IFN-α for 6 h and the relative ISRE–luciferase activity ($n = 4$) was determined as described in Materials and methods. Lane 1, transfection with 1 μg pcDNA3 without IFN-α; lane 2, transfection with 1 μg pcDNA3 with IFN-α; lanes 3, 4 and 5, transfection with 0.2, 0.5, and 0.8 μg JAB pcDNA, respectively, with IFN-α; lanes 6, 7, and 8, transfection with 0.2, 0.5, and 0.8 μg SOCS-3 pcDNA, respectively, with IFN-α. Data are expressed as means ± SD and are representative examples of three similar experiments.

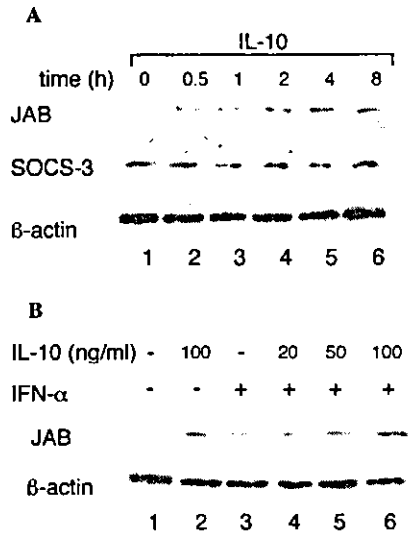

Fig. 6. Effects of IL-10 and IFN-α on JAB and SOCS-3 expression. (A) HuH-7 cells were incubated in the absence (lane 1) or presence of 100 ng/mL IL-10 for the indicated periods and expression of JAB or SOCS-3 proteins, as well as expression of β-actin as a control, was analyzed by Western blotting. (B) HuH-7 were untreated (lane 1) or treated with 100 ng/mL IL-10 (lane 2), 500 IU/mL IFN-α (lane 3) or IFN-α in combination with 20, 50, and 100 ng/mL IL-10 (lanes 4, 5, and 6, respectively) for 2 h for Western blot analysis of JAB protein or β-actin as a control.

to stimulate its expression. Moreover, IFN-α could, to some degree, induce JAB protein expression and addition of IL-10 enhanced its expression cooperatively with IFN-α (Fig. 6B).

Discussion

Recent advances in cell biology allow the identification of distinctive signaling molecules for a variety of cytokines. However, the molecular mechanisms by which many cytokines positively or negatively regulate IFN signals are not fully understood. Since clinical observations suggest the involvement of IL-1β and IL-10 in regulation of antiviral activities induced by IFNs in patients with HBV or HCV [7–9,15,16], the present study examined their effects on IFN-α signaling in HuH-7 human hepatoma cells.

Our results showed that IL-1β could not stimulate the 2′5′-OAS or PKR gene expression, but IFN-α in combination with IL-1β clearly augmented both antiviral gene expression. Consistent with this, treatment with both IFN-α and IL-1β, in comparison with IFN-α alone, resulted in enhanced stimulation of relative ISRE–luciferase activity, as well as CAT activity derived from the 2′5′-OAS gene promoter containing the ISRE-sequence, in the reporter gene transfection assay. These results were in agreement with our previous observations that IFN-α and IL-1β synergistically acted to suppress HBV enhancer-1 activity in HuH-7 cells through enhanced interaction between the ISRE-sequence in HBV enhancer-1 and ISGF3 [10,11].

Tyrosine phosphorylation of STAT1 and STAT2 is a key event for the formation and nuclear translocation of ISGF3 in response to IFN-α stimulation [25], since STATs function as a cytoplasmic retention factor for p48 without stimulation [5]. In this study, the addition of 100 IU/mL of IL-1β alone did not elicit the tyrosine phosphorylation of STAT1. However, IFN-α combined with IL-1β resulted in the tyrosine phosphorylation of STAT1 at a higher level and for a longer period than IFN-α alone in both HuH-7 and HepG2 cells, without

affecting JAK1 activation. On the other hand, Tian et al. [26] reported that IL-1β priming followed by IFN-α/β inhibits STAT1 activation in HepG2 cells by a proteasome-dependent mechanism that may target directly IFN-α/β receptors, because IL-1β did not attenuate IFN-γ-activated STAT1. Thus, this inhibition occurred at a limited time interval from IL-1β priming to IFN-α/β treatment (30–60 min) and necessitated a much higher concentration of IL-1β (>500 or 1000 IU/mL). This finding may, in part, account for the differences in the results of the two studies. We confirmed that addition of 1000 IU/mL of IL-1β, 60 min before IFN-α treatment, repressed the IFN-α-induced tyrosine phosphorylation of STAT1 in HepG2 cells as reported by Tian et al. [26] (data not shown). Tyk2 is another receptor-associated upstream kinase involved in STAT1 activation; however, the recent study using Tyk2-deficient mice indicates a restricted role of Tyk2 in IFN-α signaling [27]. In addition, IL-1β receptor does not express the intrinsic tyrosine kinase activity [28]. IL-1β cannot activate JAK1 or Tyk2 in HepG2 cells [26]. Based on these results, it is conceivable that the enhanced and sustained tyrosine phosphorylation of STAT1 induced by IFN-α combined with IL-1β is independent of activation of receptor-associated kinases. To elucidate the possible mechanism, we focused on p38 MAP kinase, since recent studies have shown that p38 can mediate STAT1 tyrosine phosphorylation irrespective of JAK1 activation [23]. In our study, IL-1β caused p38 activation as reported previously [29], and addition of SB203580, a specific inhibitor of p38, suppressed IL-1β/IFN-α-stimulated tyrosine phosphorylation of STAT1. Similarly, SB203580 abrogated the stimulatory effect of IL-1β on IFN-α-induced reporter gene activation. These results suggest that p38 is involved in IFN-α/IL-1β-induced tyrosine phosphorylation of STAT1, although p38 cannot directly activate STAT1 and protein-tyrosine kinase activity is required for this process as seen upon hyperosmotic stress [23]. STAT activation could not be only the result of increased tyrosine kinase activity but also the result of inhibition of an inactivating tyrosine phosphatase. Taken together, previous studies showed that IL-1β could inactivate a redox-sensitive protein phosphatase during the early event in the signal transduction cascade [30] and that IL-1β signaling processes may involve regulation of a protein-tyrosine phosphatase rather than a protein kinase [28]. Therefore, one possible explanation is that IL-1β inhibits a STAT1-associated protein-tyrosine phosphatase activity through the p38-mediated pathway, which is in turn involved in enhanced and prolonged STAT1 activation in response to IFN-α by stabilizing the phosphorylated STAT1, although the process remains to be clarified in future studies. In addition, we demonstrated that IFN-α and IL-1β synergistically induced the phosphorylation of STAT1 at serine-727 residue. This may, in part, account for the enhancement of IFN-α-stimulated gene expression by IL-1β, because the serine phosphorylation of STAT1 is necessary for full activation of this molecule [17].

IL-10 is an immunoregulatory cytokine known to attenuate a wide range of immune effectors and inflammatory responses [13,14,31]. In this study, IL-10 caused inhibition of IFN-α-induced expression of 2′5′-OAS and PKR genes, which was demonstrated by Northern blotting and Western blotting, respectively. In the reporter gene transfection assay, IL-10 suppressed IFN-α-activated ISRE–reporter gene expression. Moreover, Western blot analysis showed that IL-10 dose-dependently inhibited STAT1 activation induced by IFN-α. Several mechanisms responsible for inhibition of the IFN signaling pathway have been proposed. The activated JAK–STAT signaling can be reduced by dephosphorylation, proteolytic degradation, and inhibitory molecules containing a central SH2 domain and a conserved C-terminal SOCS-box, particularly JAB/SOCS-1 and CIS-3/SOCS-3 [24]. Both proteins can bind to the phosphorylated tyrosine residues on JAK proteins and inhibit the JAK-STAT signaling pathways [32–34]. In addition, induction of SOCS-3 has been implicated in IL-10-mediated suppression of IFN-α-activated STAT1 tyrosine phosphorylation in human monocytes [35] and neutrophils [36]. In our study, JAB and SOCS-3 overexpression resulted in suppression of IFN-α-stimulated ISRE–luciferase activity, in which JAB was found to be more efficient than SOCS-3. By Western blotting, HuH-7 cells expressed SOCS-3 at baseline, but IL-10 could not upregulate its expression. In contrast, IL-10 clearly induced JAB expression, and IL-10 and IFN-α cooperatively stimulated its expression, although the basal expression of JAB was almost undetectable in HuH-7 cells. Some investigators have demonstrated that JAB is a physiological negative regulator of IFN-γ-induced JAK/STAT1 activity [24] and that IFN-γ is a potent inducer of JAB in different cell types [21]. However, previous studies showed the inhibitory effects of JAB expression on the antiviral and anti-proliferative activities induced by IFN-α [21,37]. Furthermore, several studies have shown that other cytokines such as IL-6, GM-CSF, and EPO are also involved in JAB gene regulation probably through common or different cellular processes [32,34]. In accordance with these results, it is likely that JAB protein induced by IL-10 or IL-10 in combination with IFN-α contributes to suppression of the JAK–STAT signaling activated by IFN-α in HuH-7 cells, leading to inhibition of antiviral gene expression. Several lines of evidence indicate that JAB and SOCS-3 function in a negative feedback loop of cytokine signaling, especially IFN signaling [21,37]. The deregulated overexpression of JAB and SOCS-3 is believed to confer IFN-resistance to the cells, although JAB can display a much stronger inhibitory activity toward JAK–STAT activation in response to IFNs than SOCS-3

[37]. In this context, the constitutive expression of SOCS-3 and the lack of its responsiveness to IL-10 in HuH-7 cells would be linked to an aberrant regulation of JAK–STAT pathways in cancer [38].

In conclusion, we have demonstrated in the present study that IL-1β and IL-10 serve as potent modulators of IFN-α-induced antiviral gene expression in HuH-7 human hepatoma cells, although many questions remain unanswered. Understanding the interactive effects of IL-1β and IL-10 as well as other cytokines on IFN signaling pathways may lead to the development of more effective therapeutic approaches to the control of viral clearance and liver inflammation in patients with HBV and HCV.

Acknowledgments

We thank Dr. N. Fujii (Sapporo Medical University) for providing pQ6A-CAT plasmid and Dr. A. Yoshimura (Kyushu University) for providing JAB pcDNA and CIS-3 pcDNA plasmids.

References

[1] P. Tiollais, C. Pourcel, A. Dejean, The hepatitis B virus, Nature 317 (1985) 489–495.
[2] K. Kiyosawa, T. Sodeyama, E. Tanaka, Y. Gibo, K. Yoshizawa, Y. Nakano, S. Furuta, Y. Akahane, K. Nishioka, R.H. Purcell, Interrelationship of blood transfusion, non-A, non-B hepatitis and hepatocellular carcinoma: analysis by detection of antibody to hepatitis C virus, Hepatology 12 (1990) 671–675.
[3] A.H. Malik, W.M. Lee, Chronic hepatitis B virus infection: treatment strategies for the next millennium, Ann. Intern. Med. 132 (2000) 723–731.
[4] D.R. Nelson, G.Y. Lauwers, J.Y. Lau, G.L. Davis, Interleukin 10 treatment reduces fibrosis in patients with chronic hepatitis C: a pilot trial of interferon nonresponders, Gastroenterology 118 (2000) 655–660.
[5] T. Kimura, Y. Kadokawa, H. Harada, M. Matsumoto, M. Sato, Y. Kashiwazaki, M. Tarutani, R.S. Tan, T. Takasugi, T. Matsuyama, T.W. Mak, S. Noguchi, T. Taniguchi, Essential and non-redundant roles of p48 (ISGF3 gamma) and IRF-1 in both type I and type II interferon responses, as revealed by gene targeting studies, Genes Cells 1 (1996) 115–124.
[6] D. Rebouillat, A.G. Hovanessian, The human 2′,5′-oligoadenylate synthetase family: interferon-induced proteins with unique enzymatic properties, J. Interferon Cytokine Res. 19 (1999) 295–308.
[7] F.L. Dumoulin, L. Leifeld, U. Honecker, T. Sauerbruch, U. Spengler, Intrahepatic expression of interleukin-1beta and tumor necrosis factor-alpha in chronic hepatitis C, J. Infect. Dis. 180 (1999) 1704–1708.
[8] E.C. Mendoza, T.G. Paglieroni, J.B. Zeldis, Decreased phorbol myristate acetate-induced release of tumor necrosis factor-alpha and interleukin-1 beta from peripheral blood monocytes of patients chronically infected with hepatitis C virus, J. Infect. Dis. 174 (1996) 842–844.
[9] H.M. Daniels, A. Meager, A.L. Eddleston, G.J. Alexander, R. Williams, Spontaneous production of tumour necrosis factor alpha and interleukin-1 beta during interferon-alpha treatment of chronic HBV infection, Lancet 335 (1990) 875–877.
[10] K. Hamasaki, K. Nakata, K. Nakao, S. Mitsuoka, T. Tsutsumi, Y. Kato, M. Shima, N. Ishii, T. Tamaoki, S. Nagataki, Interaction of interferon-alpha with interleukin-1 beta or tumor necrosis factor-alpha on hepatitis B virus enhancer activity, Biochem. Biophys. Res. Commun. 183 (1992) 904–909.
[11] K. Nakao, K. Nakata, M. Yamashita, Y. Tamada, K. Hamasaki, H. Ishikawa, Y. Kato, K. Eguchi, N. Ishii, p48 (ISGF-3gamma) is involved in interferon-alpha-induced suppression of hepatitis B virus enhancer-1 activity, J. Biol. Chem. 274 (1999) 28075–28078.
[12] M.E. Cramp, S. Rossol, S. Chokshi, P. Carucci, R. Williams, N.V. Naoumov, Hepatitis C virus-specific T-cell reactivity during interferon and ribavirin treatment in chronic hepatitis C, Gastroenterology 118 (2000) 346–355.
[13] K. Thompson, J. Maltby, J. Fallowfield, M. McAulay, H. Millward-Sadler, N. Sheron, Interleukin-10 expression and function in experimental murine liver inflammation and fibrosis, Hepatology 28 (1998) 1597–1606.
[14] K.C. Thompson, A. Trowern, A. Fowell, M. Marathe, C. Haycock, M.J. Arthur, N. Sheron, Primary rat and mouse hepatic stellate cells express the macrophage inhibitor cytokine interleukin-10 during the course of activation in vitro, Hepatology 28 (1998) 1518–1524.
[15] S. Kakumu, A. Okumura, T. Ishikawa, K. Iwata, M. Yano, K. Yoshioka, Production of interleukins 10 and 12 by peripheral blood mononuclear cells (PBMC) in chronic hepatitis C virus (HCV) infection, Clin. Exp. Immunol. 108 (1997) 138–143.
[16] C.J. Edwards-Smith, J.R. Jonsson, D.M. Purdie, A. Bansal, C. Shorthouse, E.E. Powell, Interleukin-10 promoter polymorphism predicts initial response of chronic hepatitis C to interferon alfa, Hepatology 30 (1999) 526–530.
[17] K.C. Goh, S.J. Haque, B.R. Williams, p38 MAP kinase is required for STAT1 serine phosphorylation and transcriptional activation induced by interferons, EMBO J. 18 (1999) 5601–5608.
[18] E.B. Traenckner, S. Wilk, P.A. Baeuerle, A proteasome inhibitor prevents activation of NF-kappa B and stabilizes a newly phosphorylated form of I kappa B-alpha that is still bound to NF-kappa B, EMBO J. 13 (1994) 5433–5441.
[19] T. Ichikawa, K. Nakao, K. Nakata, K. Hamasaki, Y. Takeda, Y. Kajiya, S. Higashi, K. Ohkubo, Y. Kato, N. Ishii, K. Eguchi, Geranylgeranylacetone induces antiviral gene expression in human hepatoma cells, Biochem. Biophys. Res. Commun. 280 (2001) 933–939.
[20] P. Benech, Y. Mory, M. Revel, J. Chebath, Structure of two forms of the interferon-induced (2′–5′) oligo A synthetase of human cells based on cDNAs and gene sequences, EMBO J. 4 (1985) 2249–2256.
[21] H. Sakamoto, H. Yasukawa, M. Masuhara, S. Tanimura, A. Sasaki, K. Yuge, M. Ohtsubo, A. Ohtsuka, T. Fujita, T. Ohta, Y. Furukawa, S. Iwase, H. Yamada, A. Yoshimura, A Janus kinase inhibitor, JAB, is an interferon-gamma-inducible gene and confers resistance to interferons, Blood 92 (1998) 1668–1676.
[22] M.R. Player, P.F. Torrence, The 2–5A system: modulation of viral and cellular processes through acceleration of RNA degradation, Pharmacol. Ther. 78 (1998) 55–113.
[23] J.G. Bode, P. Gatsios, S. Ludwig, U.R. Rapp, D. Haussinger, P.C. Heinrich, L. Graeve, The mitogen-activated protein (MAP) kinase p38 and its upstream activator MAP kinase kinase 6 are involved in the activation of signal transducer and activator of transcription by hyperosmolarity, J. Biol. Chem. 274 (1999) 30222–30227.
[24] H. Yasukawa, A. Sasaki, A. Yoshimura, Negative regulation of cytokine signaling pathways, Annu. Rev. Immunol. 18 (2000) 143–164.
[25] C. Schindler, J.E. Darnell Jr., Transcriptional responses to polypeptide ligands: the JAK-STAT pathway, Annu. Rev. Biochem. 64 (1995) 621–651.
[26] Z. Tian, X. Shen, H. Feng, B. Gao, IL-1 beta attenuates IFN-alpha beta-induced antiviral activity and STAT1 activation in the liver: involvement of proteasome-dependent pathway, J. Immunol. 165 (2000) 3959–3965.

[27] K. Shimoda, K. Kato, K. Aoki, T. Matsuda, A. Miyamoto, M. Shibamori, M. Yamashita, A. Numata, K. Takase, S. Kobayashi, S. Shibata, Y. Asano, H. Gondo, K. Sekiguchi, K. Nakayama, Tyk2 plays a restricted role in IFN alpha signaling, although it is required for IL-12-mediated T cell function, Immunity 13 (2000) 561–571.

[28] D.M. Rzymkiewicz, J. DuMaine, A.R. Morrison, IL-1 beta regulates rat mesangial cyclooxygenase II gene expression by tyrosine phosphorylation, Kidney Int. 47 (1995) 1354–1363.

[29] A. Paul, S. Wilson, C.M. Belham, C.J. Robinson, P.H. Scott, G.W. Gould, R. Plevin, Stress-activated protein kinases: activation, regulation and function, Cell Signal 9 (1997) 403–410.

[30] G.R. Guy, J. Cairns, S.B. Ng, Y.H. Tan, Inactivation of a redox-sensitive protein phosphatase during the early events of tumor necrosis factor/interleukin-1 signal transduction, J. Biol. Chem. 268 (1993) 2141–2148.

[31] H. Louis, J.L. Van Laethem, W. Wu, E. Quertinmont, C. Degraef, K. Van den Berg, A. Demols, M. Goldman, O. Le Moine, A. Geerts, J. Deviere, Interleukin-10 controls neutrophilic infiltration, hepatocyte proliferation, and liver fibrosis induced by carbon tetrachloride in mice, Hepatology 28 (1998) 1607–1615.

[32] T.A. Endo, M. Masuhara, M. Yokouchi, R. Suzuki, H. Sakamoto, K. Mitsui, A. Matsumoto, S. Tanimura, M. Ohtsubo, H. Misawa, T. Miyazaki, N. Leonor, T. Taniguchi, T. Fujita, Y. Kanakura, S. Komiya, A. Yoshimura, A new protein containing an SH2 domain that inhibits JAK kinases, Nature 387 (1997) 921–924.

[33] T. Naka, M. Narazaki, M. Hirata, T. Matsumoto, S. Minamoto, A. Aono, N. Nishimoto, T. Kajita, T. Taga, K. Yoshizaki, S. Akira, T. Kishimoto, Structure and function of a new STAT-induced STAT inhibitor, Nature 387 (1997) 924–929.

[34] R. Starr, T.A. Willson, E.M. Viney, L.J. Murray, J.R. Rayner, B.J. Jenkins, T.J. Gonda, W.S. Alexander, D. Metcalf, N.A. Nicola, D.J. Hilton, A family of cytokine-inducible inhibitors of signalling, Nature 387 (1997) 917–921.

[35] S. Ito, P. Ansari, M. Sakatsume, H. Dickensheets, N. Vazquez, R.P. Donnelly, A.C. Larner, D.S. Finbloom, Interleukin-10 inhibits expression of both interferon alpha- and interferon gamma-induced genes by suppressing tyrosine phosphorylation of STAT1, Blood 93 (1999) 1456–1463.

[36] M.A. Cassatella, S. Gasperini, C. Bovolenta, F. Calzetti, M. Vollebregt, P. Scapini, M. Marchi, R. Suzuki, A. Suzuki, A. Yoshimura, Interleukin-10 (IL-10) selectively enhances CIS3/SOCS3 mRNA expression in human neutrophils: evidence for an IL-10-induced pathway that is independent of STAT protein activation, Blood 94 (1999) 2880–2889.

[37] M.M. Song, K. Shuai, The suppressor of cytokine signaling (SOCS) 1 and SOCS3 but not SOCS2 proteins inhibit interferon-mediated antiviral and antiproliferative activities, J. Biol. Chem. 273 (1998) 35056–35062.

[38] H. Yoshikawa, K. Matsubara, G.S. Qian, P. Jackson, J.D. Groopman, J.E. Manning, C.C. Harris, J.G. Herman, SOCS-1, a negative regulator of the JAK/STAT pathway, is silenced by methylation in human hepatocellular carcinoma and shows growth-suppression activity, Nat. Genet. 28 (2001) 29–35.

Antiangiogenic Gene Therapy for Hepatocellular Carcinoma Using Angiostatin Gene

Hiroki Ishikawa,[1] Kazuhiko Nakao,[2] Kojiro Matsumoto,[1] Tatsuki Ichikawa,[1] Keisuke Hamasaki,[1] Keisuke Nakata,[1] and Katsumi Eguchi[1]

Recent studies have reported that antiangiogenic gene delivery into cancer cells inhibits growth of certain tumors *in vivo*. Hepatocellular carcinoma (HCC) is a hypervascular cancer, and antiangiogenic gene therapy might be suitable for HCC. In the present study, we investigated the antiangiogenic effects of angiostatin gene transduction into HCC both *in vitro* and *in vivo*. Angiostatin gene was cloned into a pSecTag2B mammalian expression vector to construct pSecTag2B-ANG. pSecTag2B or pSecTag2B-ANG were transfected into an HCC cell line, PLC/PRF/5, and then stable transfectants were obtained by Zeocin selection. pSecTag2B or pSecTag2B-ANG transfection did not alter the expression of vascular endothelial growth factor (VEGF), a potent angiogenic stimulator, or pigment epithelium-derived factor (PEDF), an angiogenic inhibitor, in PLC/PRF/5 cells. However, conditioned media (CM) derived from pSecTag2B-ANG–transfected PLC/PRF/5 cells (CM-ANG) suppressed the proliferation and migration of human umbilical vein endothelial cells (HUVEC) by 35% and 50%, respectively, relative to their effects on nontransfected cells. In *in vivo* experiments, pSecTag2B-ANG stable transfected (CM-Mock) and nontransfected cells (CM-N) were mixed at various proportions and the mixed cells were subcutaneously implanted into athymic mice. Suppression of tumor growth was noted in mice implanted with angiostatin gene–transfected cells, and such suppression was proportional with the percentage of transfected cells. Analysis of the vascular density in these tumors showed that the tumor growth suppression effect of angiostatin gene correlated with suppression of tumor vascularity. In conclusion, antiangiogenic gene therapy using angiostatin gene is potentially suitable for the treatment of patients with HCC. (HEPATOLOGY 2003;37:696-704.)

See Editorial on Page 505

Hepatocellular carcinoma (HCC) is one of the most common malignancies worldwide and causes approximately one million deaths annually.[1,2] Several strategies have been implemented for the treatment of patients with HCC, such as surgical resection, percutaneous ethanol injection, transcatheter arterial embolization, and liver transplantation.[1,2] However, reduced hepatic reserve resulting from underlying liver cirrhosis restricts the use of these therapeutic modalities for HCC.[3] In addition, tumor recurrence rates are very high, even in patients with HCC who receive medical or surgical treatments. Therefore, a novel approach for the treatment of HCC is needed.

Gene therapy has been used for many cancers and a number of strategies have been developed for cancer gene therapy, such as transduction of suicide genes or tumor suppressor genes into cancer cells and activation of antitumor immunity by transduction of cytokine genes.[4,5] We have previously reported the effectiveness of the recombinant retroviral vectors carrying a suicide gene, HSV-tk gene, regulated by the 5′-flanking sequences of the human α-fetoprotein gene, in human HCC cells *in vitro* and *in vivo*.[6,7] On the other hand, it has recently been reported that antiangiogenic agents sufficiently inhibit tumor growth *in vivo*.[8] Because HCC is a hypervascular cancer, antiangiogenic therapy might be particularly

Abbreviations: HCC, hepatocellular carcinoma; VEGF, vascular endothelial growth factor; PEDF, pigment epithelium-derived factor; HUVEC, human umbilical endothelial cells; cDNA, complementary DNA; CM, conditioned media; CM-ANG, pSecTag2B-ANG–transfected PLC/PRF/5 cells; CM-Mock, pSecTag2B-transfected PLC/PRF/5 cells; CM-N, nontransfected PLC/PRF/5 cells; PBS-T, phosphate-buffered saline containing 0.1% Tween 20.

From the [1]First Department of Internal Medicine, Nagasaki University School of Medicine, and [2]Health Research Center, Nagasaki University, Nagasaki, Japan.

Received August 7, 2002; accepted December 3, 2002.

Address reprint requests to: Katsumi Eguchi, M.D., First Department of Internal Medicine, Nagasaki University of Medicine, 1-7-1 Sakamoto, Nagasaki, 852-8501, Japan. E-mail: jaco@venus.dti.ne.jp; fax: (81) 95-849-7270.

0270-9139/03/3703-0026$30.00/0
doi:10.1053/jhep.2003.50077

effective in the treatment of patients with HCC. However, systemic administration of antiangiogenic agents, such as thalidomide[9] or TNP-470,[10] might not be the most efficient method for locally aggressive tumors. Thus, it is conceivable that antiangiogenic gene delivery to cancer cells should be suitable for the treatment of HCC, where it can increase the local concentration of therapeutic endogenous agents.

In the present study, we constructed a mammalian expression vector that was cloned as an angiostatin gene. As previously reported, angiostatin is a potent antiangiogenic endogenous protein found in the serum and urine of mice with Lewis lung carcinoma and produced from plasminogen or plasmin.[11,12] Following stable transfection of this vector into PLC/PRF/5, an HCC cell line, we investigated the mechanism of antiangiogenic property of angiostatin by evaluating the influence of angiostatin gene transduction on the expression of vascular endothelial growth factor (VEGF) and pigment epithelium-derived factor (PEDF) in PLC/PRF/5 cells. We also investigated the effect of transfection on the proliferation and migration of cultured human umbilical vein endothelial cells (HUVEC) *in vitro* and on the progression of tumors implanted subcutaneously in nude mice *in vivo*.

Materials and Methods

Cell Culture. Human hepatoma cell line PLC/PRF/5 cells were cultured in RPMI with 10% fetal bovine serum and antibiotics at 37°C in 5% CO_2. HUVEC were purchased from Sankyo Junyaku (Tokyo, Japan) and grown in Endothelial Cell Growth Medium (EGM) medium according to the instructions provided by the supplier. HUVEC were grown to less than 6 passages for all experiments.

Plasmid Construction and Transfection. The mouse angiostatin complementary DNA (cDNA) was amplified by reverse-transcription polymerase chain reaction using mouse normal liver total RNA as the template and angiostatin-specific primers as reported previously.[13] The 1.3-kilobase mouse angiostatin cDNA was cloned into pSecTag2B mammalian expression vector (Invitrogen, Carlsbad, CA) to construct pSecTag2B-ANG. Transfection was performed using 10 μg pSecTag2B or pSecTag2B-ANG by the lipofection method (Life Technologies, Inc., Gaithersburg, MD). After transfection, the cells were then cultured in complete medium containing 100 μg/mL Zeocin for 2 weeks. Zeocin-resistant pooled populations were subjected to further studies. The transfected or nontransfected cells were further incubated at 37°C in 5% CO_2, and numbers of viable cells were counted using the trypan blue dye exclusion method for every 6 days.

Northern Blotting. Total RNA was isolated using the guanidinium isothiocyanate method. Total RNA (10 μg) was fractionated on a 1% formaldehyde agarose gel, transferred to a nylon membrane, and hybridized with [^{32}P]-labeled cDNA probes. Mouse angiostatin, human PEDF cDNA, or human VEGF were used as probes.

Western Blotting. Transfected and nontransfected PLC/PRF/5 cells ($\sim 2 \times 10^6$) were plated on 100-mm dishes. After 24 hours, the medium was replaced with 10 mL serum-free RPMI and incubated for 48 hours. Conditioned media (CM) was then derived from pSecTag2B-ANG–transfected PLC/PRF/5 cells (CM-ANG) and pSecTag2B-transfected PLC/PRF/5 cells (CM-Mock) as well as from nontransfected PLC/PRF/5 cells (CM-N). Mouse angiostatin secreted by CM-ANG was removed by using His trap kit (Amersham Life Science, Buckinghamshire, England), and the flow-through fraction (CM-ANG ΔHis) was collected. The removed hexahistidine-tagged angiostatin was eluted from His trapped column (His fraction). The same amount of each CM (15 μL) or 15 μL of 10-fold diluted His fraction was subjected to 4% to 12% sodium dodecyl sulfate/polyacrylamide gel electrophoresis. Proteins were transferred onto nitrocellulose membranes that were then blocked for 1.5 hours using 5% nonfat dried milk in phosphate-buffered saline containing 0.1% Tween 20 (PBS-T), washed with PBS-T, and incubated at room temperature for 1 hour in the presence of the antibody (rabbit polyclonal anti-hexahistidine [6his]; ICN, Costa Mesa, CA). The membranes were washed with PBS-T and incubated with horseradish peroxidase–conjugated anti-rabbit immunoglobulin G for 1 hour. Following washing with PBS-T, immunoreactive bands were visualized by the enhanced chemiluminescence system (Amersham Life Science).

VEGF Enzyme-Linked Immunosorbent Assay. One milliliter of each derived CM was lyophilized with Speed-Vac (Savant, Farmingdale, NY) and resuspended in 100 μL phosphate-buffered saline. VEGF concentration was assayed using the Quantikine HS Human VEGF Immunoassay Kit (R&D Systems, Minneapolis, MN) according to the manufacturer's instructions.

Cell Proliferation Assay and Migration Assay of HUVEC. HUVEC were plated onto 24-well culture plates at $\sim 5 \times 10^4$ cells/well for 24 hours. Medium was then replaced with equal aliquots of CM derived from cultures of transfected or nontransfected PLC/PRF/5 cells. In the method of coculture, instead of replacement with CM, 8.0 μm Transwells (Corning, Acton, MA) with 1×10^5 cells of nontransfected or transfected PLC/PRF/5 cells were placed onto each well. After 48 hours, HUVEC

were trypsinized and counted. On the other hand, migration was measured with the 8.0-μm Transwells as described previously with some modifications.[14] Briefly, 600 μL of each CM sample was placed in the lower chamber and then incubated at 37°C for 30 minutes before addition of HUVEC into the upper chamber. Subconfluent 16-hour cultures of HUVEC in the growth factor–free medium were harvested, washed, and resuspended in serum-free RPMI. HUVEC (~2 × 10^5) in 100 μL serum-free RPMI were added to the upper chamber. After 24 hours of incubation, all nonmigrating cells were removed from the upper surface of the membrane with a cotton swab; cells that had migrated to the lower surface were fixed with absolute methanol, stained with Giemsa, and photographed. For quantitative analysis, stained cells were subsequently extracted with 10% acetic acid and absorbance was determined at 595 nm. All experiments were performed in triplicate.

Animal Experiments. Four-week-old male BALB/c nu/nu athymic mice were purchased from Charles River (Yokohama, Japan). Animal experiments were performed in accordance with institutional guidelines, and the study was approved by the ethics committee of Nagasaki University. The angiostatin gene stable transfected PLC/PRF/5 cells and nontransfected PLC/PRF/5 cells were mixed at various proportions (0%, 10%, 50%, and 100% of transfectants), and 1 × 10^6 mixed cells were subcutaneously implanted into the right thigh of athymic mice. Each group consisted of 5 mice. Serial changes in tumor volume were estimated based on the Battelle Columbus Laboratory protocol with the following formula at 3-day intervals after inoculation for 8 weeks:

$$VT\ (mm^3) = L \times W^2 \times \tfrac{1}{2}$$

where VT is the estimated tumor volume and L and W are length (mm) and width (mm) of the transplanted tumor, respectively, measured with vernier calipers over the skin. In mice that did not develop tumors in the subcutaneous region (see Results), postmortem examination was conducted at 8 weeks after inoculation of angiostatin gene stable transfected PLC/PRF/5 cells to confirm the absence of such tumors.

Immunohistochemistry. Immunohistochemistry was performed using anti-mouse angiostatin and anti-mouse CD31 antibodies. Tissue samples of the tumor extracted from each mouse were cut into 4-μm-thick sections and mounted on aminopropyltriethoxysilane-coated glass slides. The streptavidin-biotin method (Histofine Staining Kit; Nichirei Co., Tokyo, Japan) was used for immunohistochemical detection as described previously.[15] Briefly, endogenous peroxidase was inactivated by immersing the section in 3% hydrogen peroxide solution.

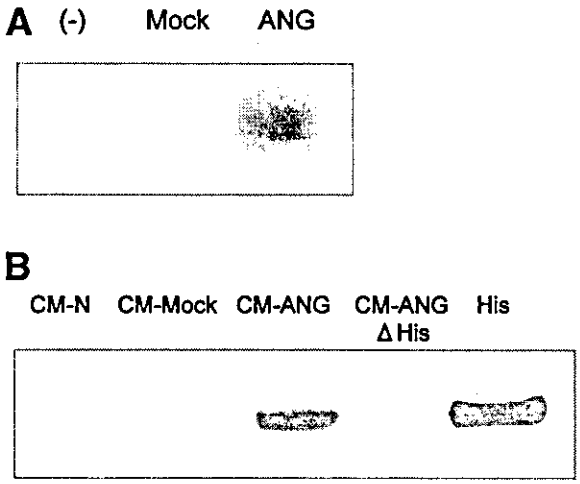

Fig. 1. Expression of angiostatin in pSecTag2B-ANG-transfected PLC/PRF/5 cells. (A) Total RNA was extracted from Zeocin-selected transfected or nontransfected PLC/PRF/5 cells. The 1.3-kilobase band indicates angiostatin gene messenger RNA. (−), nontransfected; Mock, pSecTag2B-transfected; ANG, pSecTag2B-ANG-transfected PLC/PRF/5 cells. (B) CM was collected after 48-hour incubation of each cell type in serum-free CM. The expression of angiostatin protein was analyzed by Western blotting in each CM using anti-hexahistidine antibody.

Sections were incubated with rabbit anti-mouse angiostatin antibody (Yanaihara Institute Inc., Shizuoka, Japan) or rabbit anti-mouse CD31 antibody (Santa Cruz Biotechnology, Santa Cruz, CA) in a humidified chamber for 60 minutes at room temperature. The sections were next incubated with the appropriate biotinylated anti-rabbit antibody for 30 minutes, washed, and incubated with peroxidase-conjugated streptavidin. Color was developed using 3,3′-diaminobenzidine and hydrogen peroxide. Anti-mouse angiostatin antibody–treated slides were counterstained with hematoxylin.

Statistical Analysis. All data were expressed as mean ± SD. Differences between groups were examined for statistical significance using Student's t test. All reported P values are 2 tailed, and those less than .01 were considered statistically significant.

Results

Establishment of Stable Transfectant of the Angiostatin Gene. We constructed the mammalian expression vector in which the angiostatin gene was tagged to hexahistidine (pSecTag2B-ANG). The human hepatoma cell line, PLC/PRF/5, was transfected with pSecTag2B or pSecTag2B-ANG, and total RNA was extracted from Zeocin-resistant cells. Northern blot analysis showed 1.3-kilobase angiostatin messenger RNA in pSecTag2B-ANG–transfected PLC/PRF/5 cells (Fig. 1A). In

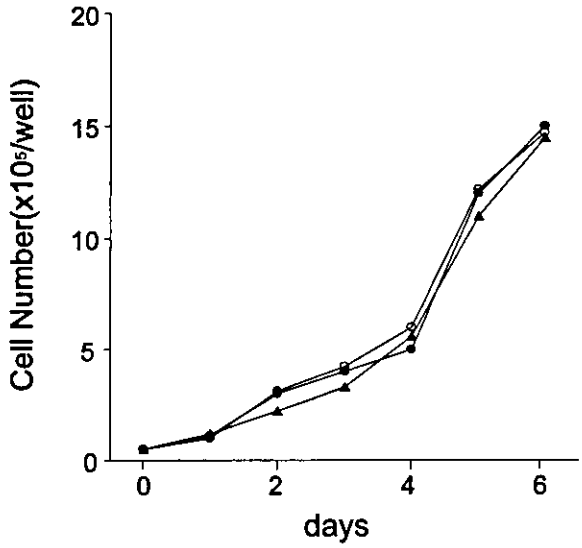

Fig. 2. Growth of transfected or nontransfected PLC/PRF/5 cells. The transfected or nontransfected cells were incubated at 37°C in 5% CO_2, and numbers of viable cells were counted using the trypan blue dye exclusion method every 6 days. The results shown are the mean of 3 separate experiments. ●, pSecTag2B-ANG-transfected cells; ▲, pSecTag2B-transfected cells; ■, nontransfected PLC/PRF/5 cells.

addition, CM-ANG contained the angiostatin protein tagged with hexahistidine, as detected by Western blotting using anti-hexahistidine antibody (Fig. 1B). Angiostatin messenger RNA expression was not detected in nontransfected and pSecTag2B-transfected PLC/PRF/5 cells. Furthermore, angiostatin protein was not detected in CM-N, CM-Mock, and CM-ANG ΔHis. His fraction eluted through the His trap system contained a sufficient amount of angiostatin protein tagged with hexahistidine. The proliferation of PLC/PRF/5 cells was not influenced by pSecTag2B or pSecTag2B-ANG stable transfection (Fig. 2).

Influence of Angiostatin Gene Transduction on PEDF and VEGF Expression. Gao et al.[16] reported that plasminogen kringle-5 up-regulated the expression of PEDF and down-regulated the expression of VEGF in vascular cells of the retina. Because the mechanism of antiangiogenic activity of angiostatin remains unclear, we used plasminogen kringle 1-4 (which is identified by angiostatin) to investigate the influence of angiostatin gene transduction on the expression of PEDF and VEGF (Fig. 3). PEDF messenger RNA was not constitutively expressed in PLC/PRF/5 cells, and pSecTag2B or pSecTag2B-ANG transfection did not stimulate its expression. In addition, the messenger RNA of VEGF and soluble VEGF in the CM were not altered by stable pSecTag2B or pSecTag2B-ANG transfection. On the other hand, the concentration of soluble VEGF was not different in CM-ANG ΔHis compared with CM-ANG (CM-N, 1.21 ± 0.22; CM-Mock, 1.15 ± 0.23; CM-ANG, 1.20 ± 0.09; CM-ANG ΔHis, 1.11 ± 0.28 ng/mL).

Suppression of Proliferation and Migration of HUVEC. HUVEC were cultured in each CM or cocultured with transfected or nontransfected PLC/PRF/5 cells using a double chamber, and their numbers were determined 48 hours later (Fig. 4). CM-ANG inhibited the proliferative activity by 35% compared with CM-N

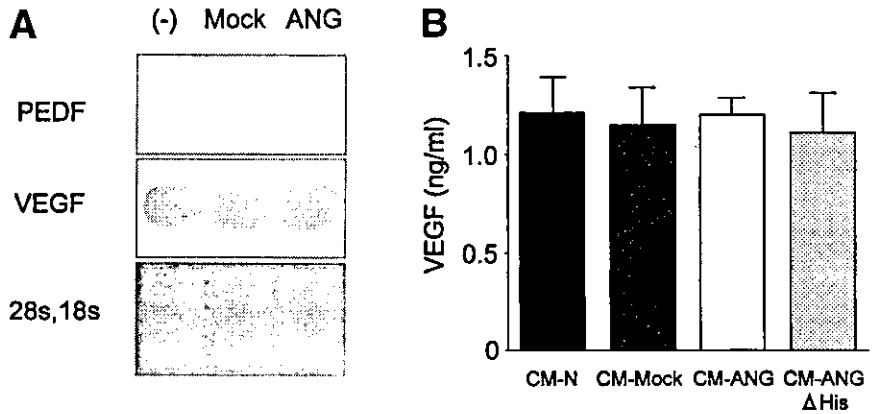

Fig. 3. Expression of PEDF and VEGF in transfected and nontransfected PLC/PRF/5 cells. (A) Total RNA was extracted from transfected or nontransfected PLC/PRF/5 cells. Northern analysis was performed with PEDF and VEGF specific probes. (−), nontransfected; Mock, pSecTag2B-transfected cells; ANG, pSecTag2B-ANG-transfected PLC/PRF/5 cells. The **lower panel** shows 28S and 18S ribosomal RNA as internal controls. (B) VEGF concentrations in CM derived from transfected or nontransfected PLC/PRF/5 cells. pSecTag2B-ANG, pSecTag2B-transfected, or nontransfected PLC/PRF/5 cells were incubated in serum-free RPMI for 48 hours and aliquots of CM were collected. VEGF concentration was measured by enzyme-linked immunosorbent assay. Data represent the mean ± SD of 3 separate experiments.

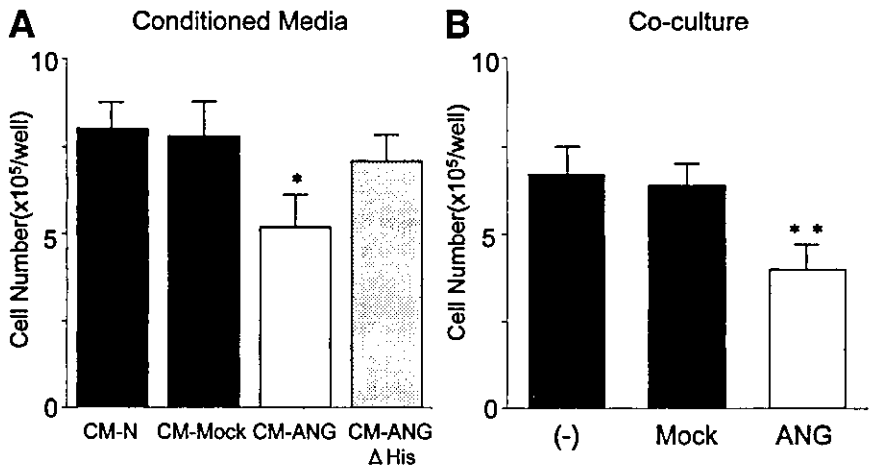

Fig. 4. Endothelial cell proliferation. (A) HUVEC were cultured on 48-well culture plates in 500 μL CM derived from transfected or nontransfected PLC/PRF/5 cells. Cell numbers were determined after 48-hour incubation. *$P < .01$ vs. CM-N, CM-Mock, and CM-ANG ΔHis. (B) HUVEC proliferation was also evaluated with coculture method described in Materials and Methods. After coculture for 48 hours, cell numbers were determined. (−), nontransfected cells; Mock, pSecTag2B-transfected cells; ANG, pSecTag2B-ANG-transfected PLC/PRF/5 cells. Data represent the mean ± SD of 3 separate experiments. **$P < .01$ vs. nontransfected or Mock.

(CM-N, 8.0 ± 0.7 × 10^5/well; CM-Mock, 7.8 ± 0.9 × 10^5/well; CM-ANG, 5.2 ± 0.9 × 10^5/well; CM-ANG ΔHis, 7.1 ± 0.7 × 10^5/well; $P < .01$; Fig. 4A). Coculture of HUVEC with pSecTag2B-ANG–transfected PLC/PRF/5 cells resulted in suppression of HUVEC proliferation by 40% compared with nontransfected PLC/PRF/5 cells (CM-N, 6.7 ± 0.6 × 10^5/well; CM-Mock, 6.4 ± 0.5 × 10^5/well; CM-ANG, 4.0 ± 0.7 × 10^5/well; $P < .01$; Fig. 4B). CM-Mock, CM-ANG ΔHis, and coculture with pSecTag2B-ANG–transfected PLC/PRF/5 cells did not influence HUVEC proliferation. We also used the modified Boyden chamber assay to investigate the migration of HUVEC (Fig. 5). CM derived from transfected or nontransfected PLC/PRF/5 cells was placed in the lower chambers, and HUVEC were plated in the upper chamber. CM-ANG suppressed the migration of HUVEC through membrane pores (Fig. 5A). Quantitative analysis showed that the migration-suppressive effects of CM-

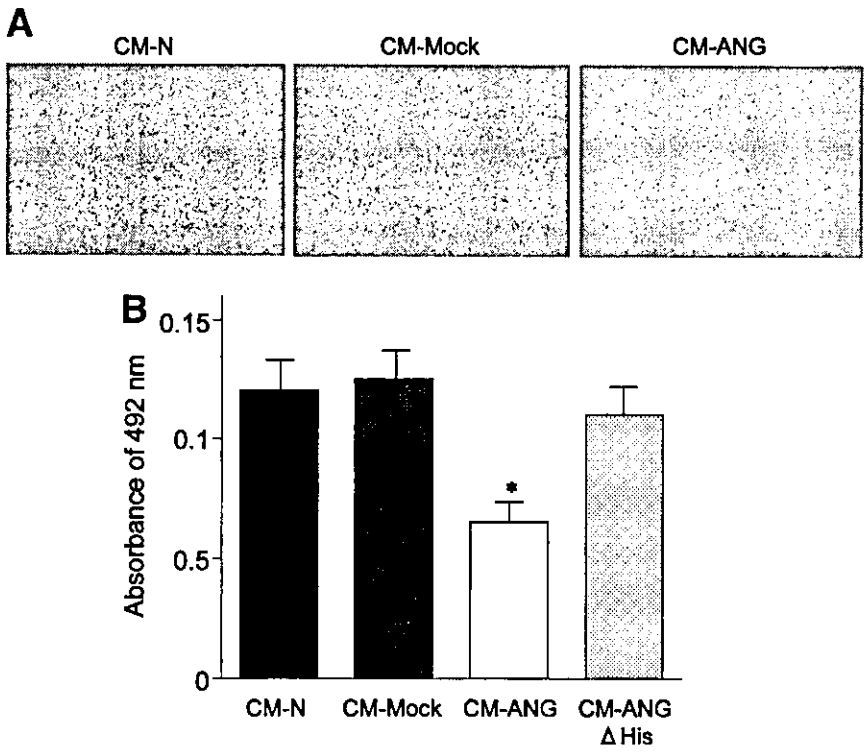

Fig. 5. Migration of HUVEC in a modified Boyden chamber assay. The sample CM was placed in the lower chamber, and HUVEC were added to the upper chamber of a modified Boyden chamber. After 24-hour incubation, nonmigrating cells were removed and cells that migrated through the membrane pores (8 μm) were stained with Giemsa and photographed. (A) Representative micrographs of migrated HUVEC in CM-N, CM-Mock, or CM-ANG (original magnification ×40). (B) Quantification of migrated cells. Stained cells were extracted with 10% acetic acid, and absorbance of extracted solution was determined. Data are mean ± SD of 3 separate experiments. *$P < .01$ vs. CM-N, CM-Mock, and CM-ANG ΔHis.